3-2023

Hedging cryptos with Bitcoin futures

Francis LIU

Natalie PACKHAM

Meng-Jou LU

Wolfgang Karl HAERDLE
Singapore Management University

Hedging Cryptos with Bitcoin Futures

Francis Liu*

Natalie Packham†

Meng-Jou Lu ‡

Wolfgang Karl Härdle§¶

This version: December 16, 2021

Abstract

The introduction of derivatives on Bitcoin enables investors to hedge risk exposures in cryptocurrencies. Because of volatility swings and jumps in cryptocurrency prices, the traditional variance-based approach to obtain hedge ratios is infeasible. As a consequence, we consider two extensions of the traditional approach: first, different dependence structures are modelled by different copulae, such as the Gaussian, Student-t, Normal Inverse Gaussian and Archimedean copulae; second, different risk measures, such as value-at-risk, expected shortfall and spectral risk measures are employed to find the optimal hedge ratio. Extensive out-of-sample tests give insights in the practice of hedging various cryptos and crypto indices, including Bitcoin, Ethereum, Cardano, the CRIX index and a number of crypto-portfolios in the time period December 2017 until May 2021. Evidences show that BTC futures can effectively hedge BTC and BTC-involved indices. This promising result is consistent across different risk measures and copulae except for Frank. On the other hand, we observe complex and diverse dependence structures between BTC-not-involved assets and the futures. As a consequence, results of hedging other assets and indices are diverse and, in some occasions, not ideal.

JEL classification: G11, G13

Keywords: Cryptocurrencies, risk management, hedging, copulas

*Department of Business and Economics, Berlin School of Economics and Law, Badensche Str. 52, 10825 Berlin, Germany. Blockchain Research Center, Humboldt-Universität zu Berlin, Germany. International Research Training Group 1792, Humboldt-Universität zu Berlin, Germany. E-mail: Francis.Liu@hwr-berlin.de.

†Department of Business and Economics, Berlin School of Economics and Law, Badensche Str. 52, 10825 Berlin, Germany. International Research Training Group 1792, Humboldt-Universität zu Berlin, Germany. E-mail: packham@hwr-berlin.de.

‡Department of Finance, Asia University, 500, Lioufeng Rd., Wufeng, Taichung 41354, Taiwan Department of Finance, Asia University, 500, Lioufeng Rd., Wufeng, Taichung 41354, Taiwan E-mail: mangrou@gmail.com.

§Blockchain Research Center, Humboldt-Universität zu Berlin, Germany. Wang Yanan Institute for Studies in Economics, Xiamen University, China. Sim Kee Boon Institute for Financial Economics, Singapore Management University, Singapore. Faculty of Mathematics and Physics, Charles University, Czech Republic. National Yang Ming Chiao Tung University, Taiwan. E-mail: haerdle@wiwi.hu-berlin.de.

¶Financial support of the European Union's Horizon 2020 research and innovation program "FIN-TECH: A Financial supervision and Technology compliance training programme" under the grant agreement No 825215 (Topic: ICT-35-2018, Type of action: CSA), the European Cooperation in Science & Technology COST Action grant CA19130 - Fintech and Artificial Intelligence in Finance - Towards a transparent financial industry, the Deutsche Forschungsgemeinschaft's IRTG 1792 grant, the Yushan Scholar Program of Taiwan the Czech Science Foundation's grant no. 19-28231X / CAS: XDA 23020303 are greatly acknowledged.

1 Introduction

Cryptocurrency (CC) is a fast-growing asset class, Over 7,000 cryptos[1] are now available on the market since the first cryptocurrency Bitcoin (BTC) surfaced (Nakamoto, 2009). In response to the rapid development of the CC market, the CME Group launched exchange-traded BTC futures contracts in December 2017. At the time of writing, the CME BTC futures is the only regulated cryptos futures in the market. The average daily volume and open interest of the CME BTC futures are $2,518 million and $2,836 million respectively. The BTC futures is an attractive derivative for investor to participate in the crypto market as it is legal, standardised and well-understood.

More individual and institutional investors are adding CCs and CC derivatives into their portfolios, creating the need to understand downside risks and find suitable ways to hedge against extreme risks. Fom a risk management perspective, the roller-coaster ride of crypto prices creates significant basis risk, even when using simple hedges involving crypto portfolios and BTC futures. This requires analysing the dependence structure of cryptos and futures beyond linear correlation.

In this paper, we analyse static hedges of crypto portfolios with Bitcoin futures. Owing to the asymmetry of crypto returns as well as the occurrence of extreme events, we consider different dependence structures via a variety of copula models and we optimise the hedge ratio using different risk measures. A similar study was conducted by (Barbi and Romagnoli, 2014) for equity and FX portfolios. Barbi and Romagnoli (2014)'s work is based on Cherubini et al. (2011) to derive the distribution of linear combination of margins with copula as their dependence structure. We slightly amend their lemma and come up with a formula for the linear combination of random variables for our purpose.

The hedge ratio is the appropriate amount of futures contracts to be held in order to eliminate risk exposure in the underlying security. The determination of the optimal hedge ratio relies primarily on the dependence between the underlying cryptos and futures prices. Copulae provide the flexibility to model multivariate random variables separately by their margins and dependence structure. The concept of copulae was originally developed (but not under this name) by Wassily Hoeffding (Hoeffding, 1940a) and later popularised by the work of Abe Sklar (Sklar, 1959).

Different risk measures account for investors' risk attitudes. They serve as loss functions in the searching process of the optimal hedge ratio. Of the vast literature discussed the relationship between risk measures and investor's risk attitude, we refer readers to Artzner et al. (1999) for an axiomatic, economic reasoning approach of risk measure construction; Embrechts et al. (2002) for reasoning of using Expected Shortfall (ES) and Spectral Risk Measures (SRM) in addition to VaR; Acerbi (2002) for direct linkage between risk measures and investor's risk attitude using the concept of a "risk aversion function".

Financial asset returns have long known to be non-Gaussian, see e.g. (Fama, 1963; Cont, 2001). Specifically, Gaussian models cannot produce the heavy tails and the asymmetry observed in asset returns, which in turn implies a consistent underestimation of financial risks. Therefore, to minimize down risk, one cannot solely rely on second-order moment calculations. Moreover, variance as a risk measure does not account for the variety of investors' utility functions. In particular, it is known that investors are tail-risk averse, see Menezes et al. (1980).

In order to capture a variety of risk preferences, in addition to variance, we include the risk measures value-at-risk (VaR), expected shortfall (ES), and spectral risk measures (SRM). VaR is widely used by the finance industry and easy to understand. ES and SRM are chosen because of their coherence property, in particular, they recognize diversification benefits. SRM can also be directly related to

[1]Data from statista (https://bit.ly/3GADIxB).

an individual's utility function. Examples are the exponential SRM and power SRM introduced by Dowd et al. (2008).

In the empirical part of this work, we study the hedging effectiveness of the Bitcoin futures to various cryptos and crypto indices under different risk preferences. With an extensive back-test [2] , we find the ability of the BTC futures to hedge BTC and BTC-related indices promising regardless of copula (except Frank copula) and risk measures. On the other hand, the results of BTC futures to hedge other cryptos and indices are diverse.

This paper is organized as follows. Section 2 introduces the notion of optimal hedge ratio; section 3 decribes the method of estimation of copulae; section 4 provides the empirical result; section 5 concludes. All calculations in this work can be reproduced. The results are reproducible with data and codes available on www.quantlet.com .

2 Optimal hedge ratio

2.1 Distribution of hedge portfolio

We form a portfolio with two assets, a spot asset and a futures contract, for example Bitcoin spot and a CME Bitcoin futures contract. Our objective is to minimize the risk of the exposure in the spot. To keep a simple portfolio setting, we go long one unit of the spot and short h units of the future, $h \geq 0$. Letting R^S and R^F be the (discrete) returns of the spot and futures price. The (discrete) return of the portfolio is[3]

$$R^h = R^S - hR^F.$$

If the portfolio reduces the risk of the spot position, then we call this a hedge portfolio. To measure risk, we define a risk measures ρ to be a mapping from a financial position, such as R^h, to a real number, which is often interpreted as the amount of money to make the position acceptable (e.g. to a regulator), see e.g. (Föllmer and Schied, 2002).

An optimal hedge ratio (OHR) h^* is a parameter that minimizes the risk of the aforementioned portfolio

$$h^* = \underset{h}{\operatorname{argmin}}\, \rho(R^h).$$

For example, Value-at-Risk (VaR) at the confidence level α is the absolute value of the $1-\alpha$-quantile of R^h, i.e., $\mathrm{VaR}_{1-\alpha} = -F^{(-1)}_{R^h}(1-\alpha) = -\inf\{x \in \mathbb{R} : 1-\alpha \leq F_{R^h}(x)\}$, where F_{R^h} is the distribution function of R^h.

Obviously the cdf of R^h and the risk measure depend on the joint distribution of R^S and $-hR^F$.

Optimising h according to $f_{R^S,-hR^F}$ is unfavorable in the sense that one would need to calibrate the joint pdf $f_{R^S,-hR^F}$ whenever updating h. Another problem of using the joint pdf is that one lacks the flexibility to model the margins separately from the dependence structure. To overcome both of these problems, we use copulae.

The benefit of using copulae is two fold. First, copulae are invariant under strictly monotone increasing function (Schweizer et al., 1981), see the Lemma below. Second, copulae allow us to model the margins and dependence structure separately, see Sklar's Theorem (Sklar, 1959). See also (Nelsen, 1999; Joe, 1997; McNeil et al., 2005) for Sklar's Theorem.

[2]We apprepciate the data provider Tiingo (https://www.tiingo.com/) for the valuable crypto prices data.

[3]This is equivalent to stating that if both the spot price S_{t-1} and the futures price F_{t-1} are normalised to 1, then h units of the future will hedge the value change $\Delta V = \Delta S - h\Delta F$, where $\Delta S = S_t - S_{t-1}$, etc.

Theorem 1 (Hoeffding Sklar Theorem) *Let F be a joint distribution function with margins F_X, F_Y. Then, there exists a copula $C : [0,1]^2 \mapsto [0,1]$ such that, for all $x, y \in \mathbb{R}$*

$$F(x,y) = C\{F_X(x), F_Y(y)\}. \tag{1}$$

If the margins are continuous, then C is unique; otherwise C is unique on the range of the margins.

Conversely, if C is a copula and F_X, F_Y are univariate distribution functions, then the function F defined by (1) is a joint distribution function with margins F_X, F_Y.

Indeed, many basic results about copulae can be traced back to early works of Wassily Hoeffding (Hoeffding, 1940b, 1941). The works aimed to derive a measure of relationship of variables, which is invariant under change of scale. See also Fisher and Sen (2012) for English translations of the original papers written in German.

Lemma 1

$$C_{X,hY}\left(F_X(s), F_{hY}(t)\right) = C_{X,Y}\left(F_X(s), F_Y(t/h)\right). \tag{2}$$

Proof. Since copulae are invariant under strictly monotone increasing function (Schweizer et al., 1981, Theorem 3 (i)),

$$C_{X,hY}\left(F_X(s), F_{hY}(t)\right) = C_{X,Y}\left(F_X(s), F_{hY}(t)\right).$$

We rewrite second argument of the copula

$$\begin{aligned} F_{hY}(t) &= \mathbb{P}(hY \leq t) \\ &= \mathbb{P}(Y \leq t/h) \\ &= F_Y(t/h), \end{aligned}$$

and finish the proof. ■

Leveraging these two features of copulae, Barbi and Romagnoli (2014) introduce the distribution of linear combinations of random variables using copulae. We slightly edit the Corollary 2.1 of their work and yield the following expression of the distribution.

Proposition 2 *Let X and Y be two real-valued continuous random variables on a probability space $(\Omega, \mathcal{F}, \mathbf{P})$ with absolutely continuous copula $C_{X,Y}$ and marginal distribution functions F_X and F_Y. Then, the distribution function of Z is given by*

$$F_Z(z) = 1 - \int_0^1 D_1 C_{X,Y}\left[u, F_Y\left\{\frac{F_X^{(-1)}(u) - z}{h}\right\}\right] du. \tag{3}$$

Here, $F^{(-1)}$ denotes the inverse of F, i.e., the quantile function.

Here $D_1 C(u,v) = \dfrac{\partial}{\partial u} C(u,v)$ and, see e.g. Equation (5.15) of (McNeil et al., 2005),

$$D_1 C_{X,Y}\{F_X(x), F_Y(y)\} = \mathbf{P}(Y \leq y | X = x). \tag{4}$$

Proof. Using the identity (4) gives

$$F_Z(z) = \mathbf{P}(X - hY \leq z) = \mathbb{E}\left\{\mathbf{P}\left(Y \geq \frac{X-z}{h}\Big|X\right)\right\}$$

$$= 1 - \mathbb{E}\left\{\mathbf{P}\left(Y \leq \frac{X-z}{h}\Big|X\right)\right\} = 1 - \int_0^1 D_1 C_{X,Y}\left[u, F_Y\left\{\frac{F_X^{(-1)}(u) - z}{h}\right\}\right] du.$$

■

Corollary 1 *Given the formulation of random variables, the pdf of Z can be written as*

$$f_Z(z) = \left|\frac{1}{h}\right| \int_0^1 c_{X,Y}\left[F_Y\left\{\frac{F_X^{(-1)}(u) - z}{h}\right\}, u\right] \cdot f_Y\left\{\frac{F_X^{(-1)}(u) - z}{h}\right\} du, \tag{5}$$

or

$$f_Z(z) = \int_0^1 c_{X,Y}\left[F_X\left\{z + hF_Y^{(-1)}(u)\right\}, u\right] \cdot f_X\left\{z + hF_Y^{(-1)}(u)\right\} du. \tag{6}$$

The two expressions are equivalent. Note that the pdf of Z in the above proposition can be assessed via numerical integration as long as we have the copula density and the marginal densities. A generic expression and proof can be found in the appendix.

2.2 Procedure to determine optimal hedge ratio

We introduce the empirical procedure to obtain the optimal hedge ratio (OHR) being used in this work. First, we split the time series of spot and futures into sets of training and testing data. The training data makes up the first 300 observations and its corresponding testing data consists of the consecutive 5 observations. We then roll 5 observations forward (step size of 5) to obtain the next training and test data sets and repeat this until the end of the time series. Note that the testing data are non-overlapping since the step size and equal to test size.

Next, we obtain the OHR as follows:

1. **Construct Univariate Kernel Density Function (KDE)**. From the training data we calibrate the spot and futures' univariate kernel density functions using the Gaussian kernel with bandwidth determined by the refined plug-in method (Härdle et al., 2004, section 3.3.3).

2. **Calibrate Copulae**. We then calibrate the copulae outlined in section 3.1 via the method of moments described in section 3.2.1.

3. **Select Copula**. We compute the Akaike Information Criterion. The copula with the best (i.e., lowest) AIC is used for the next step. A discussion of this step is found in 3.2.3.

4. **Determine OHR**. We determine the OHRs numerically using different risk measures as the loss function by drawing samples from the selected copula and KDEs. The risk measures used as risk reduction objectives are outlined in 3.3

5. **Obtain testing log-return of hedged portfolio**. Finally, we apply the OHRs to the test data $R_h = R_s - h^* R_f$.

3 Copulae and risk measures

3.1 Copulae

To capture different aspects of the dependence structure, we consider a number of different copulas, which are layed out in details below Gaussian-, t-, Frank-, Gumbel-, Clayton-, mixture, NIG factor, and Plackett-copula.

As this hedging exercise concerns only portfolios with two assets, we focus on the bivariate version of copulae and some important features of a copula, including Kendall's τ_K and Spearman's ρ_S.

Kendall's τ and Spearman's ρ are measures of association in terms of concordance, see Kruskal (1958) Let (x_i, y_i) and (x_j, y_j) denote two observations from a vector (X, Y) of continuous random variables. A pair of observations is concordant if $x_i < x_j$ and $y_i < y_j$, discordant if $x_i > x_j$ and $y_i < y_j$ or if $x_i < x_j$ and $y_i > y_j$. For a bivariate random variable of n observations, there are $\binom{n}{2}$ distinct pairs.

Let c denote the number of concordant pairs, and d the number of discordant pairs, Kendall's tau is defined as follows (Nelsen, 1999)

$$\tau_K \stackrel{\text{def}}{=} \frac{c-d}{c+d}$$

$$= \frac{c-d}{\binom{n}{2}};$$

Let F_X and F_Y be cdfs of X and Y respectively, Spearman's ρ is

$$\rho_S \stackrel{\text{def}}{=} 12\mathbb{E}(F_X(X)F_Y(Y)) - 3;$$

Upper tail dependence is defined as

$$\lambda_U \stackrel{\text{def}}{=} \lim_{q \to 1^-} \mathbf{P}\{X > F_X^{(-1)}(q) | Y > F_Y^{(-1)}(q)\};$$

Lower tail dependence is defined as

$$\lambda_L \stackrel{\text{def}}{=} \lim_{q \to 0^+} \mathbf{P}\{X \leq F_X^{(-1)}(q) | Y \leq F_Y^{(-1)}(q)\}.$$

Furthermore, we denote the Fréchet-Hoeffding lower bound by $\boldsymbol{W}$, the product copula by $\boldsymbol{\Pi}$, and the Fréchet-Hoeffding upper bound by $\boldsymbol{M}$. They represent cases of perfect negative dependence, independence, and perfect positive dependence, respectively. For further details, we refer readers to Joe (1997) and Nelsen (1999); see also Härdle and Okhrin (2010).

The symmetry property of copulae is also important for modelling financial data. In particular, we are interested in the radially symmetric among other symmetry definitions, see Nelsen (1999).

Definition 3 *Let $(U_1, ..., U_d)$ be random variables. The random variables is radially symmetric if the joint cdf of $(U_1, ..., U_d)$ is same as the joint cdf of $(1 - U_1, ..., 1 - U_d)$*

To illustrate the difference among copulae, we plot random samples drawn from copulae listed below in figure 1.

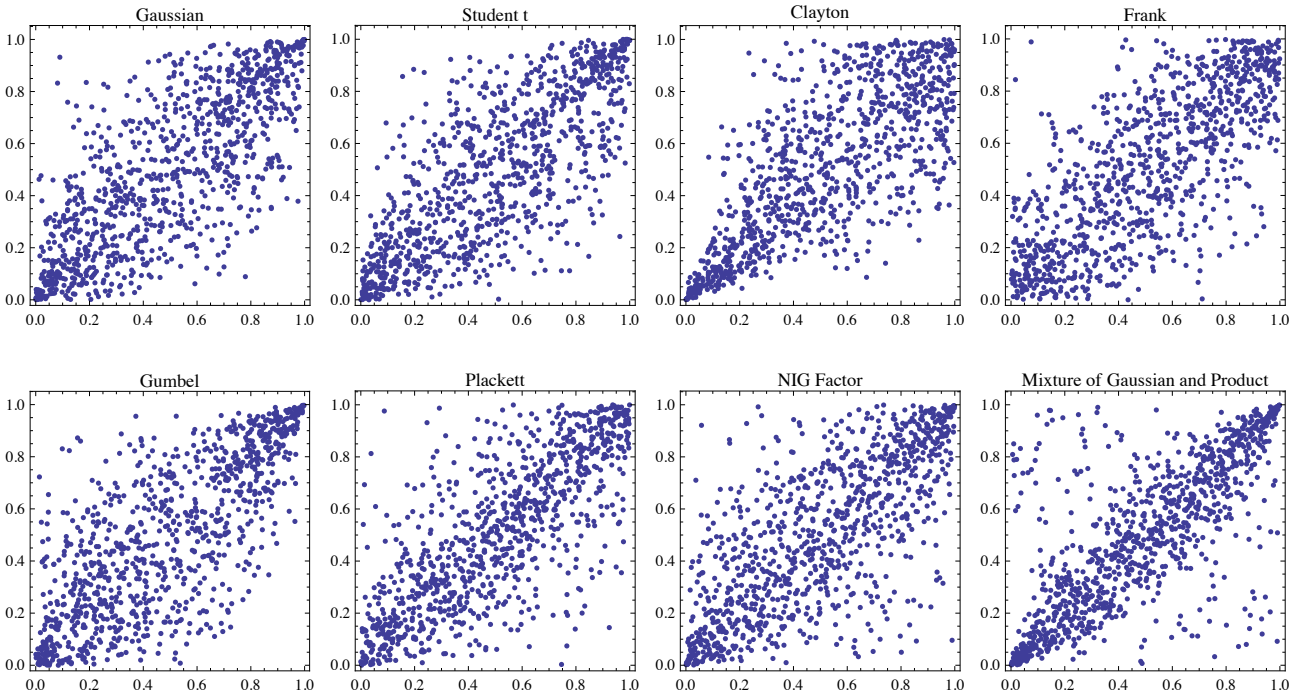

Figure 1: Scatterplots of samples drawn from copulae. All copulae are calibrated to Spearman's ρ of 0.75 before sampling.

3.1.1 Gaussian and t Copulae

Gaussian and t copulae are dervived from Gaussian and t distributions. Since Gaussian and t distributions are elliptical distributions, Gaussian and t copulae are called elliptical copulae.

Gaussian copula (bivariate) is defined as

$$\begin{aligned}\boldsymbol{C}(u,v) &= \Phi_{2,\rho}\{\Phi^{(-1)}(u), \Phi^{(-1)}(v)\} \\ &= \int_{-\infty}^{\Phi^{(-1)}(u)} \int_{-\infty}^{\Phi^{(-1)}(v)} \frac{1}{2\pi\sqrt{1-\rho^2}} \exp\left\{\frac{s^2 - 2\rho st + t^2}{2(1-\rho^2)}\right\} \mathrm{d}s\,\mathrm{d}t,\end{aligned}$$

where $\Phi_{2,\rho}$ is the cdf of bivariate Normal distribution with zero mean, unit variance, and correlation coefficient ρ, and $\Phi^{(-1)}$ is the quantile function univariate standard normal distribution.

Note that we use ρ to denote the correlation parameter as well as a $\rho(\cdot)$ to denote a risk measure.

The Gaussian copula is fully specified by the correlation parameter ρ. Like all elliptical copulas, it is symmetric. It has no tail dependence, which, in a finance context, implies that it often underestimates tail risk.

The Gaussian copula density is

$$\begin{aligned}\boldsymbol{c}_\rho(u,v) &= \frac{\boldsymbol{\varphi}_{2,\rho}\{\Phi^{(-1)}(u), \Phi^{(-1)}(v)\}}{\varphi\{\Phi^{(-1)}(u)\} \cdot \varphi\{\Phi^{(-1)}(v)\}} \\ &= \frac{1}{2\pi\sqrt{1-\rho^2}} \exp\left\{-\frac{u^2 - 2\rho uv + v^2}{2(1-\rho^2)}\right\},\end{aligned}$$

where $\boldsymbol{\varphi}_{2,\rho}(\cdot)$ is the pdf corresponding to $\Phi_{2,\rho}$, and $\varphi(\cdot)$ the standard normal distribution pdf.

Kendall's τ_K and Spearman's ρ_S of a bivariate Gaussian copula are

$$\tau_K(\rho) = \frac{2}{\pi} \arcsin \rho$$

$$\rho_S(\rho) = \frac{6}{\pi} \arcsin \frac{\rho}{2}.$$

The t-copula has the form

$$\begin{aligned} \boldsymbol{C}(u, v) &= \boldsymbol{T}_{2,\rho,\nu}\{T_\nu^{(-1)}(u), T_\nu^{(-1)}(v)\} \\ &= \int_{-\infty}^{T_\nu^{(-1)}(u)} \int_{-\infty}^{T_\nu^{(-1)}(v)} \frac{\Gamma\left(\frac{\nu+2}{2}\right)}{\Gamma\left(\frac{\nu}{2}\right) \pi\nu\sqrt{1-\rho^2}} \\ &\left(1 + \frac{s^2 - 2st\rho + t^2}{\nu}\right)^{-\frac{\nu+2}{2}} dsdt, \end{aligned}$$

where $\boldsymbol{T}_{2,\rho,\nu}$ denotes the cdf of bivariate t distribution with dependence parameter ρ and degrees of freedom parameter ν, and where $T_\nu^{(-1)}(\cdot)$ is the quantile function of a standard t distribution with degree of freedom ν.

Contrary to the Gaussian copula, the t-copula has a non-zero tail dependence coefficient, which makes it more appropriate for dependence modelling in finance. The Gaussian copula arises as $\nu \to \infty$.

The copula density is

$$\boldsymbol{c}(u, v) = \frac{\boldsymbol{t}_{2,\rho,\nu}\{T_\nu^{(-1)}(u), T_\nu^{(-1)}(v)\}}{t_\nu\{T_\nu^{(-1)}(u)\} \cdot t_\nu\{T_\nu^{(-1)}(v)\}},$$

where $\boldsymbol{t}_{2,\rho,\nu}$ is the pdf of $\boldsymbol{T}_{2,\rho,\nu}$ and t_ν the density of standard t distribution.

Like all the other elliptical copulae, the t-copula's Kendall's τ is identical to that of the Gaussian copula (see Demarta and McNeil, 2005, and references therein).

3.1.2 Archimedean copulae

The family of Archimedean copulae forms a large class of copulae with many convenient features. Contrary to elliptical copulas, which are derived from elliptical distributions. Archimedean copulas are determined via a simple parametric form of the dependence structure. A prominent feature is the ability to model asymmetric dependence structures.

In general, they take a form

$$\boldsymbol{C}(u, v) = \psi^{(-1)}\{\psi(u), \psi(v)\},$$

where $\psi : [0, 1] \to [0, \infty)$ is a continuous, strictly decreasing and convex function such that $\psi(1) = 0$ for any permissible dependence parameter θ. ψ is also called generator. $\psi^{(-1)}$ is the inverse of the generator.

The Frank copula (B3 in Joe (1997)) is a radial symmetric copula and cannot produce any tail

dependence. It takes the form

$$\boldsymbol{C}_\theta(u,v) = \frac{1}{\theta}\log\left\{1 + \frac{(e^{-\theta u}-1)(e^{-\theta v}-1)}{e^{-\theta}-1}\right\}$$

where $\theta \in [0,\infty]$ is the dependency parameter. $\boldsymbol{C}_{-\infty} = \boldsymbol{M}$, $\boldsymbol{C}_1 = \boldsymbol{\Pi}$, and $\boldsymbol{C}_\infty = \boldsymbol{W}$.

The Copula density is

$$\boldsymbol{c}_\theta(u,v) = \frac{\theta e^{\theta(u+v)(e^\theta-1)}}{\left\{e^\theta - e^{\theta u} - e^{\theta v} + e^{\theta(u+v)}\right\}^2}$$

Frank copula has Kendall's τ and Spearman's ρ as follow:

$$\tau_K(\theta) = 1 - 4\frac{D_1\{-\log(\theta)\}}{\log(\theta)},$$

and

$$\rho_S(\theta) = 1 - 12\frac{D_2\{-\log(\theta)\} - D_1\{\log(\theta)\}}{\log(\theta)},$$

where D_1 and D_2 are the Debye function of order 1 and 2. Debye function is $D_n = \frac{n}{x^n}\int_0^x \frac{t^n}{e^t-1}dt$.

The Gumbel copula (B6 in Joe (1997)) has upper tail dependence with the dependence parameter $\lambda^U = 2 - 2^{\frac{1}{\theta}}$ and displays no lower tail dependence.

$$\boldsymbol{C}_\theta(u,v) = \exp -\{(-\log(u))^\theta + (-\log(v))^\theta\}^{\frac{1}{\theta}},$$

where $\theta \in [1,\infty)$ is the dependence parameter.

While the Gumbel copula cannot model perfect counter-dependence (Nelsen, 2002), $\boldsymbol{C}_1 = \boldsymbol{\Pi}$ models the independence, and $\lim_\theta^\infty \boldsymbol{C}_\theta = \boldsymbol{W}$ models the perfect dependence. The copula density takes the form

$$\tau_K(\theta) = \frac{\theta-1}{\theta}.$$

The Clayton copula, by contrast to Gumbel copula, generates lower tail dependence of the form $\lambda^L = 2^{-\frac{1}{\theta}}$, but cannot generate upper tail dependence. The Clayton copula takes the form

$$\boldsymbol{C}_\theta(u,v) = \left\{\max(u^{-\theta} + v^{-\theta} - 1, 0)\right\}^{-\frac{1}{\theta}},$$

where $\theta \in (-\infty,\infty)$ is the dependence parameter. Moreover, $\lim_\theta^{-\infty} \boldsymbol{C}_\theta = \boldsymbol{M}$, $\boldsymbol{C}_0 = \boldsymbol{\Pi}$, and $\lim_\theta^\infty \boldsymbol{C}_\theta = \boldsymbol{W}$. Kendall's τ of the Clayton copula is given by

$$\tau_K(\theta) = \frac{\theta}{\theta+2}.$$

3.1.3 Mixture Copula

The mixture copula is a linear combination of copulae. For a 2-dimensional random variable $\boldsymbol{X} = (X_1, X_2)^\top$, its distribution can be written as linear combination of K copulae

$$\boldsymbol{C}(u,v) = \sum_{k=1}^{K} p^{(k)} \cdot \boldsymbol{C}^{(k)}\{F_{X_1}^{(-1)}(u), F_{X_2}^{(-1)}(v); \boldsymbol{\theta^{(k)}}\}.$$

The copula density is again a linear combination of copula densities

$$\boldsymbol{c}(u,v) = \sum_{k=1}^{K} p^{(k)} \cdot \boldsymbol{c}^{(k)}\{F_{X_1}^{(-1)}(u), F_{X_2}^{(-1)}(v); \boldsymbol{\theta^{(k)}}\}.$$

While Kendall's τ of mixture copula is not known in closed form, Spearman's ρ is specified by the following statement.

Proposition 4 *Let $\rho_S^{(k)}$ be Spearman's ρ of the k-th component Spearman's ρ of the mixture copula is given by*

$$\rho_S = \sum_{k=1}^{K} p^{(k)} \cdot \rho_S^{(k)}$$

Proof. Since Spearman's ρ is defined as (Nelsen, 1999)

$$\rho_S = 12 \int_{\mathbb{I}^2} \boldsymbol{C}(s,t) ds dt - 3,$$

Spearman's ρ of the the mixture copula is given by summation of the components

$$\rho_S = 12 \int_{\mathbb{I}^2} \sum_{k=1}^{K} p^{(k)} \cdot \boldsymbol{C}^{(k)}(s,t) ds dt - 3.$$

■

An example of a mixture copula is the Fr'echet class of copulas, which are given by convex combinations of $\boldsymbol{W}$, $\boldsymbol{\Pi}$, and $\boldsymbol{M}$ (Nelsen, 1999).

We use a mixture of Gaussian and independent copulas in our analysis, i.e.,

$$\boldsymbol{C}(u,v) = p \cdot \boldsymbol{C}^{\text{Gaussian}}(u,v) + (1-p)(uv),$$

with corresponding density is

$$\boldsymbol{c}(u,v) = p \cdot \boldsymbol{c}^{\text{Gaussian}}(u,v) + (1-p).$$

This mixture models the amount of "random noise" that appears in the dependence structure. In the hedging exercise, the "random noise" adds an unhedgable component to the two-asset portfolio, whose weight $(1-p)$ is calibrated from market data.

3.1.4 NIG factor copula

The *normal inverse Gaussian (NIG)* distribution, introduced by (Barndorff-Nielsen, 1997), has density function

$$g(x;\alpha,\beta,\mu,\delta) = \frac{\alpha}{\pi} \mathbf{e}^{\delta\sqrt{\alpha^2-\beta^2}-\beta\mu} \frac{1}{q((x-\mu)/\delta)} K_1\left[\delta\alpha q\left(\frac{x-\mu}{\delta}\right)\right] \mathbf{e}^{\beta x}, \quad x > 0,$$

where $q(x) = \sqrt{1+x^2}$ and where K_1 is the modified Bessel function of third order and index 1. The parameters satisfy $0 \leq |\beta| \leq \alpha$, $\mu \in \mathbb{R}$ and $\delta > 0$. The parameters have the following interpretation: μ and δ are location and scale parameters, respectively, α determines the heaviness of the tails and β

determines the degree of asymmetry. If $\beta = 0$, then the distribution is symmetric around μ.

The moment-generating function of the NIG distribution is given by

$$M(u; \alpha, \beta, \mu, \delta) = \exp\left(\delta\left(\sqrt{\alpha^2 - \beta^2} - \sqrt{\alpha^2 - (\beta + u)^2}\right) + \mu u\right).$$

As a direct consequence, moments are easily calculated with the expectation and variance of the NIG distribution being

$$\mathbb{E}X = \mu + \frac{\delta\beta}{\sqrt{\alpha^2 - \beta^2}}$$

$$\mathrm{Var}(X) = \frac{\alpha^2\delta}{(\alpha^2 - \beta^2)^{3/2}}. \tag{7}$$

The NIG$(\alpha, \beta, \mu\,\delta)$ distribution belongs to the class of so-called *normal variance-mean mixture*, (see Section 3.2 of (McNeil et al., 2005)): X follows an NIG$(\alpha, \beta, \mu, \delta)$ distribution if X conditional on W follows a normal distribution with mean $\mu + \beta W$ and variance W, i.e.,

$$X|W \overset{\mathcal{L}}{\sim} \mathrm{N}(\mu + \beta W, W),$$

where W follows an *inverse Gaussian distribution*, denoted by IG$(\delta, \sqrt{\alpha^2 - \beta^2})$.

It is easily seen from the moment-generating function that the NIG distribution is preserved under linear combinations, provided the variables share the parameters α and β. For this and other reasons, the NIG distribution is popular in many areas of financial modelling; for example, it gives rise to the normal inverse Gaussian Lévy process, which may be represented as a Brownian motion with a time change.

In the setting here, we consider the *NIG factor copula*. This is not directly derived from the multivariate NIG distribution, but determined through a factor structure instead. The factor structure, which was applied e.g. in (Kalemanova et al., 2007) for calibrating CDO's, gives additionaly flexibility as it does not force the components to have a mixing variable W. The following proposition introduces the NIG factor model and some of its properties.

Proposition 5 *Let $Z \sim NIG(\alpha, \beta, \mu, \delta)$ and $Z_i \sim NIG(\alpha, \beta, \mu_i, \delta_i)$, $i = 1, \ldots, n$ be independent NIG-distributed random variables. Then:*

1. $X_i = Z + Z_i \sim NIG(\alpha, \beta, \mu + \mu_i, \delta + \delta_i)$,
2. *and*

$$\begin{aligned} Cov(X_i, X_j) &= Var(Z), \\ Corr(X_i, X_j) &= \frac{\delta}{\sqrt{(\delta + \delta_i)(\delta + \delta_j)}}. \end{aligned} \tag{8}$$

Proof.

1. This follows directly from the moment-generating function.

2. For the covariance,

$$\begin{aligned}\mathrm{Cov}(X_i, X_j) &= \mathbb{E}[(Z + Z_i)(Z + Z_j)] - \mathbb{E}[Z + Z_i]\mathbb{E}[Z + Z_j] \\ &= \mathbb{E}[Z^2] - (\mathbb{E}Z)^2.\end{aligned}$$

The correlation is determined directly from 7.

■

The NIG factor copula is obtained by transforming the margins to uniforms (see Sklar's Theorem), giving (e.g. (Krupskii and Joe, 2013)):

$$C_{r^S,r^F}(F_{r^S}(r^S), F_{r^F}(r^F)) = \int_{\mathbb{R}} F_{Z_1}(F_{X_1}^{(-1)} \circ F_{r^S}(r^S) - z) \cdot F_{Z_2}(F_{X_2}^{(-1)} \circ F_{r^F}(r^F) - z) \cdot f_Z(z)dz$$

If the margins are continuous, then Spearman's rho of NIG factor copula is

$$\rho_S = 12 \int\int\int_{\mathbb{R}^3} F_{X_1}(x_1) \cdot F_{X_2}(x_2) \cdot f_{Z_1}(x_1 - z) \cdot f_{Z_2}(x_2 - z) \cdot f_Z(z)dx_1dx_2dz - \frac{1}{48}.$$

3.1.5 Plackett copula

The Plackett copula has an expression

$$\boldsymbol{C}_\theta(u, v) = \frac{1 + (\theta - 1)(u + v)}{2(\theta - 1)} - \frac{\sqrt{\{1 + (\theta - 1)(u + v)\}^2 - 4uv\theta(\theta - 1)}}{2(\theta - 1)}$$

$$\rho_S(\theta) = \frac{\theta + 1}{\theta - 1} - \frac{2\theta \log \theta}{(\theta - 1)^2}$$

We include Placket copula in our analysis as it possesses a special property, the cross-product ratio is equal to the dependence parameter

$$\begin{aligned}&\cdot \frac{\mathbf{P}(U \le u, V \le v) \cdot \mathbf{P}(U > u, V > v)}{\mathbf{P}(U \le u, V > v) \cdot \mathbf{P}(U > u, V \le v)} \\ &= \frac{\boldsymbol{C}_\theta(u, v)\{1 - u - v + \boldsymbol{C}_\theta(u, v)\}}{\{u - \boldsymbol{C}_\theta(u, v)\}\{v - \boldsymbol{C}_\theta(u, v)} \\ &= \theta. \end{aligned} \tag{9}$$

That is, the dependence parameter is equal to the ratio between number of concordence pairs and number of discordence pairs of a bivariate random variable.

3.2 Calibration and selection of copulae

We introduce the method to calibrate copulae to our data in this section. In general, there are two types of calibration procedures to calibrate copulae: maximum likelihood (MLE) and method of moments (MM). We decide to deploy the latter since it calibrates according to the moments desired.

In the following subsection, we present the configuration of the method of moments procedures in this work. In the subsection after, we argue that MM is more suitable to this work by comparing MM with MLE.

3.2.1 Method of moments

We trace back the usage of MM to calibrate copulae to Genest (1987); Genest and Rivest (1993). The moments mainly refer to Kendall's τ or Spearman's ρ. We extend MM to quantile dependence measures denoted by λ_q for quantile level q.

Spearman's ρ, Kendall's τ, and quantile dependence of the copula C are defined as

$$\begin{aligned}
\rho_S &= 12 \int\int_{I^2} C_{\boldsymbol{\theta}}(u,v)\,\mathrm{d}u\,\mathrm{d}v - 3 \\
\tau_K &= 4\mathbb{E}[C_{\boldsymbol{\theta}}\{F_X(x), F_Y(y)\}] - 1, \\
\lambda_q &= \begin{cases} \mathbf{P}(F_X(X) \le q | F_Y(Y) \le q) = \dfrac{C_{\boldsymbol{\theta}}(q,q)}{q}, & \text{if } q \in (0, 0.5], \\ \mathbf{P}(F_X(X) > q | F_Y(Y) > q) = \dfrac{1 - 2q + C_{\boldsymbol{\theta}}(q,q)}{1-q}, & \text{if } q \in (0.5, 1). \end{cases}
\end{aligned}$$

The empirical counterparts are

$$\begin{aligned}
\hat{\rho}_S &= \frac{12}{n}\sum_{k=1}^{n} \hat{F}_X(x_k)\hat{F}_Y(y_k) - 3, \\
\hat{\tau}_K &= \frac{4}{n}\sum_{k=1}^{n} \hat{C}\{\hat{F}_X(x_i), \hat{F}_X(y_i)\} - 1, \\
\hat{\lambda}_q &= \begin{cases} \dfrac{1}{n}\displaystyle\sum_{k=1}^{n} \frac{\mathbf{1}_{\{\hat{F}_X(x_k) \le q, \hat{F}_Y(y_k) \le q\}}}{q}, & \text{if } q \in (0, 0.5], \\ \dfrac{1}{n}\displaystyle\sum_{k=1}^{n} \frac{\mathbf{1}_{\{\hat{F}_X(x_k) > q, \hat{F}_Y(y_k) > q\}}}{1-q}, & \text{if } q \in (0.5, 1), \end{cases}
\end{aligned}$$

where $\hat{F}(x) = \dfrac{1}{n}\displaystyle\sum_{k=1}^{n} 1_{\{x_i \le x\}}$ and $\hat{C}(u,v) = \dfrac{1}{n}\displaystyle\sum_{k=1}^{n} 1_{\{u_i \le u, v_i \le v\}}$.

Denote by $\boldsymbol{m}(\boldsymbol{\theta})$ the m-dimensional vector of dependence measures according the dependence parameters $\boldsymbol{\theta}$,and let $\hat{\boldsymbol{m}}$ be the corresponding empirical counterpart. The difference between dependence measures and their counterpart is denoted by

$$\boldsymbol{g}(\boldsymbol{\theta}) = \hat{\boldsymbol{m}} - \boldsymbol{m}(\boldsymbol{\theta}).$$

The MM estimator is

$$\hat{\boldsymbol{\theta}} = \underset{\boldsymbol{\theta} \in \boldsymbol{\Theta}}{\operatorname{argmin}}\, \boldsymbol{g}(\boldsymbol{\theta})^\top \hat{\boldsymbol{W}} \boldsymbol{g}(\boldsymbol{\theta}),$$

where $\hat{W}$ is some positive definite weight matrix. In this work, we use $\boldsymbol{m}(\boldsymbol{\theta}) = (\rho_S, \lambda_{0.05}, \lambda_{0.1}, \lambda_{0.9}, \lambda_{0.95})^\top$ for calibration. $\hat{W}$ is set to identity matrix.

3.2.2 Comparison between method of moments and maximum likelihood

By the Hoeffding-Sklar theorem, the joint density of a d-dimensional random variable $\boldsymbol{X}$ with sample size n can be written as

$$\boldsymbol{f_X}(x_1, ..., x_d) = \boldsymbol{c}\{F_{X_1}(x_1), ..., F_{X_d}(x_d)\} \prod_{j=1}^{d} f_{X_i}(x_i).$$

We follow the treatment of MLE documented in section 10.1 of Joe (1997), namely the *inference functions for margins (IFM) method.* The log-likelihood $\sum_{i=1}^{n} f_{\boldsymbol{X}}(X_{i,1}, ..., X_{i,d})$ can be decomposed into a dependence part and a marginal part,

$$\begin{aligned} L(\boldsymbol{\theta}) &= \sum_{i=1}^{n} \boldsymbol{c}\{F_{X_1}(x_{i,1}; \boldsymbol{\delta}_1), ..., F_{X_d}(x_{i,d}; \boldsymbol{\delta}_d); \boldsymbol{\gamma}\} + \sum_{i=1}^{n}\sum_{j=1}^{d} f_{X_j}(x_{i,j}; \boldsymbol{\delta}_j) \\ &= L_C(\boldsymbol{\delta}_1, ..., \boldsymbol{\delta}_d, \boldsymbol{\gamma}) + \sum_{j=1}^{d} L_j(\boldsymbol{\delta}_j) \end{aligned}$$

where $\boldsymbol{\delta}_j$ are the parameters of the j-th margin, $\boldsymbol{\gamma}$ is the parameter of the parametric copula, and $\boldsymbol{\theta} = (\boldsymbol{\delta}_1, ..., \boldsymbol{\delta}_d, \boldsymbol{\gamma})$. Instead of searching the $\boldsymbol{\theta}$ in a high dimensional space, Joe (1997) suggests to search for $\hat{\boldsymbol{\delta}}_1, ..., \hat{\boldsymbol{\delta}}_d$ that maximize $L_1(\boldsymbol{\delta}_1), ..., L_d(\boldsymbol{\delta}_d)$, then search for $\hat{\boldsymbol{\gamma}}$ that maximize $L_C(\hat{\boldsymbol{\delta}}_1, ..., \hat{\boldsymbol{\delta}}_d, \boldsymbol{\gamma})$.

We follow Genest et al. (1995) who suggest to replace the estimation of marginals parameters estimation by non-parameteric estimation. Given non-parametric estimator $\hat{F}_i$ of the margins F_i, the estimator of the dependence parameters $\boldsymbol{\gamma}$ is

$$\hat{\boldsymbol{\gamma}} = \underset{\boldsymbol{\gamma}}{\operatorname{argmax}} \sum_{i=1}^{n} \boldsymbol{c}\{\hat{F}_{X_1}(x_{i,1}), ..., \hat{F}_{X_d}(x_{i,d}); \boldsymbol{\gamma}\}.$$

Both the simulated method of moments and the maximum likelihood estimation are unbiased. The question though which procedure is more suitable for hedging.

Figure 2 shows the empirical quantile dependence of Bitcoin and CME future and the copula implied quantile dependence of the MLE and MM calibration procedures. Although the MLE is a better fit to a range of quantile dependence in the middle, it fails to address the situation in the tails. We find that our data empirically has low quantile dependence in the lower ends ($q < 10\%$). We argue that MM is preferred as it produces a better fit to the dependence structure in the tail behaviour, contrary to MLE.

Therefore, we deploy the method of moments throughout the analysis. We choose the 5^{th}-, 10^{th}-, 90^{th}-, 95^{th}-quantile, and Spearman's ρ as the moments.

3.2.3 Copula selection

The dependence structure of price data changes across time, in which both the dependency parameters and the type of dependence. For this reason, we allow for a flexible choice of the best-fitting copula, by re-calibrating periodically and re-evaluating performance of the various copulas. We select the best-fitting copula, characterised by the lowest *Akaike Information Criterion (AIC)*,

$$\text{AIC} = 2k - 2\log(L),$$

where k is the number of estimated parameteres and L is the likelihood (Akaike, 1973).

Other model selection criteria, such as the TIC (Takeuchi, 1976) or likelihood ratio test could be used instead. For a survey of model selection and inference, see Anderson et al. (1998). Among various copula selection procedures, AIC is a popular choice for its applicability, see e.g. Breymann et al. (2003). In our case, the AICs are calculated only with dependency likelihood since the marginals are modelled via kernel density estimators. The selected copula will then be enter the calculation of the optimal hedge ratio.

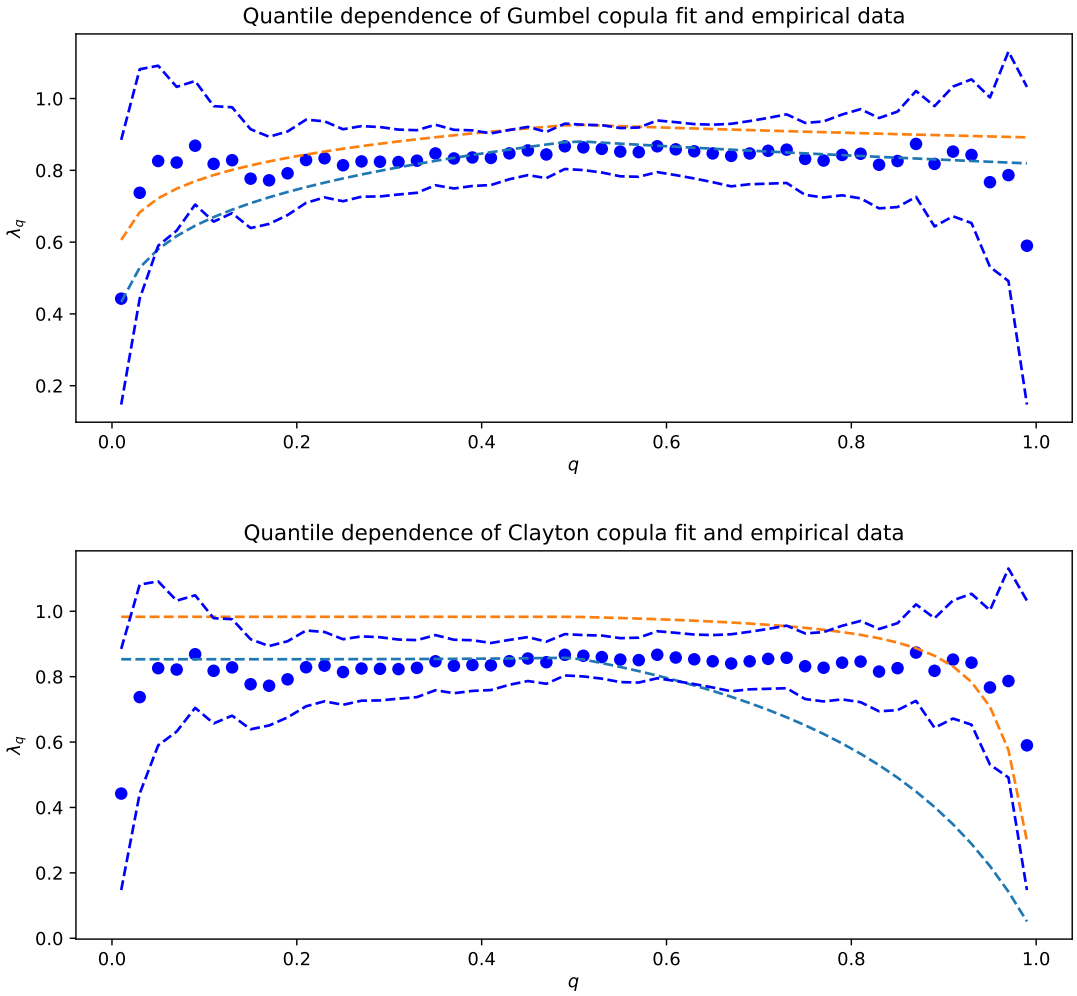

Figure 2: Quantile dependences of Gumbel, and Clayton Copula. The blue circle dots are the quantile dependence estimates of Bitcoin and CME future, blue dotted lines are the estimates' 90% confidence interval. Orange dotted line is the copula implied quantile dependence by MM estimation. Light blue dotted line is the copula implied quantile dependence by MLE estimation.

3.3 Risk measures

The optimal hedge ratio is determined for the following variety of risk measures: variance, Value-at-Risk (VaR), Expected Shortfall (ES), and Exponential Risk Measure (ERM). A summary of risk measures being used in portfolio selection problem can be found in Härdle et al. (2008). The risk measures here serve as risk minimization objectives, i.e. loss functions for searching the optimal hedge ratio.

The risk measures are defined as follows. Let Z be a random variable with distribution function F_Z.

1. Variance: $\mathrm{Var}(Z) = \mathbb{E}[(Z - \mathbb{E}Z)^2]$.
2. VaR at confidence level α: $\mathrm{VaR}_\alpha(Z) = -F_Z^{(-1)}(1-\alpha)$
3. ES at confidence level α: $\mathrm{ES}(F_Z) = -\frac{1}{1-\alpha}\int_0^{1-\alpha} F_Z^{(-1)}(p)dp$

4. ERM with Arrow-Pratt coefficient of absolute risk aversion k:

$$\mathrm{ERM}_k(F_Z) = \int_0^{1-\alpha} \phi(p) F_Z^{(-1)}(p) dp,$$

where ϕ is a weight function described in (3.3) below.

VaR, ES, and ERM fall into the class of spectral risk measures (SRM), which have the from (Acerbi, 2002)

$$\rho_\phi(r^h) = -\int_0^1 \phi(p) F_Z^{(-1)}(p) dp,$$

where p is the loss quantile and $\phi(p)$ is a user-defined weighting function defined on $[0, 1]$. We consider only so-called admissible risk spectra $\phi(p)$, i.e., fulfilling

(i) ϕ is positive,

(ii) ϕ is decreasing,

(iii) and $\int \phi = 1$.

The VaR's $\phi(p)$ gives all its weight on the $1-\alpha$ quantile of Z and zero elsewhere, i.e. the weighting function is a Dirac delta function, and hence it violates the (ii) property of admissible risk spectra. The ES' $\phi(p)$ gives all tail quantiles the same weight of $\dfrac{1}{1-\alpha}$ and non-tail quantiles zero weight. The ERM assumes investors' risk preference are in the form of an exponential utility function $U(x) = 1 - e^{kx}$, so its corresponding risk spectrum is defined as

$$\phi(p) = \frac{k e^{-k(1-p)}}{1 - e^{-k}},$$

where k is the Arrow-Pratt coefficient of absolute risk aversion. The parameter k has an economic interpretation as being the ratio between the second derivative and first derivative of investor's utility function on an risky asset,

$$k = -\frac{U''(x)}{U'(x)},$$

for x in all possible outcomes. In case of the exponential utility, k is the the constant absolute risk aversion (CARA).

4 Empirical Results

4.1 Data

In the empirical analysis, we consider the risk reduction capability of CME Bitcoin Futures (BTCF) on five cryptos, namely Bitcoin (BTC), Ethereum (ETH), Cardano (ADA), Litecoin (LTC) and Ripple (XRP), as well as five crypto indexes, namely BITX, BITW100, CRIX, BITW20, and BITW70. ETH, ADA, LTC, and XRP are popular cryptos tradable in various exchanges and have large market capitalization. BITX, BITW100, and CRIX are market-cap weighted crypto indexes with BTC as constituent. BITX and BITW100 track the total return of the 10 and 100 cryptos with largest market-cap, respectively. CRIX decides the number of constituents by AIC and tracks that number of cryptos with largest market-cap. In our case, the number of constituents in CRIX is 5. BITW20 is also a market-cap weighted crypto index but with the 20 largest market-cap cryptos outside the

constituents of BITX. BITW70 has the same construction as BITW20 but with the 70 largest market-cap cryptos outside BITX and BITW20. Therefore, BTC is excluded as a constituent in BITW20 and BITW70.

For each of the 10 hedging portfolios, a crypto or index is considered as the spot and held in a unit size long position, while the front BTCF is held in a short position with units corresponding to the OHR in order to reduce the risk of the spot. Except for the hedge of BTC, all hedging portfolios are considered to be cross-asset hedges.

We collect the spots' and BTCF's daily prices at 15:00 US Central Time (CT). The reason for choosing this particular time is that the CME group determines the daily settlements for BTCF's based on the trading activities on CME Globex between 14:59 and 15:00 CT. This is also the reporting time of the daily closing price by Bloomberg. The crypto spot data is collected from the data provider called Tiingo (https://www.tiingo.com/). Tiingo aggregates crypto OHLC (open, high, low, and close) prices fed by APIs from various exchanges. It covers major exchanges, such as Binance, Gemini, Poloniex etc., so Tiingo's aggregated OHLC price is a good representation a tradable market price. For each crypto, we match the opening price at 15:00 CT from Tiingo with the daily BTCF closing price from Bloomberg. Since CRIX is not available at 15:00 CT, we recalculated an hourly CRIX using the monthly constituents weights and the hourly OHLC price data collected from Tiingo. BITX, BITW20, BITW70, and BITW100 are collected from the official website of their publisher Bitwise.com. The daily reporting time of the Bitwise indexes is 15:00 CT.

At the time of writing, the CRIX is undergoing the listing process on the S&P Dow Jones Indices, the official CRIX data will then be calculated with Lukka Prime Data and available to the public via S&P.

4.2 Overview of the out-of-sample data

For every asset and hedge portfolio, we concatenate the out-of-sample data to form a time series for analysis. The date range of the out-of-sample time series is from 2019-10-21 to 2021-05-27, in total of 405 data points in each time series. We analyse these time series throughout the whole result section.

We introduce the out-of-sample data in this subsection before we proceed to analysing the hedged portfolio results. Figure 3 presents the BTC and BTCF price in USD in the first panel and the arithmetic difference between the daily return of BTC and BTCF, i.e. $R_s - R_f$, in the second panel. In the first panel, the black vertical lines with capital letter labels indicate the days of the five most negative daily return of BTC during out-pf-sample period. Table 1 summarizes the relevant news headlines and events of those days.

Figures 4 and 5 are the cumulative returns of the indices and individual cryptos respectively. The black vertical lines labeled by assets name are the largest daily price drop of the assets in the out-of-sample data.

The out-of-sample data covers the pre-COVID19 period, 2019-10-21 to 2020-03-09, as well as the COVID19 period, 2019-03-19 onwards. We can observe an overall upward trend of crypto prices in both periods. Nonetheless, the volatilities of assets are high (annualized around 100%) regardless of COVID19.

4.3 An overview of the hedged portfolios without the copula selection step

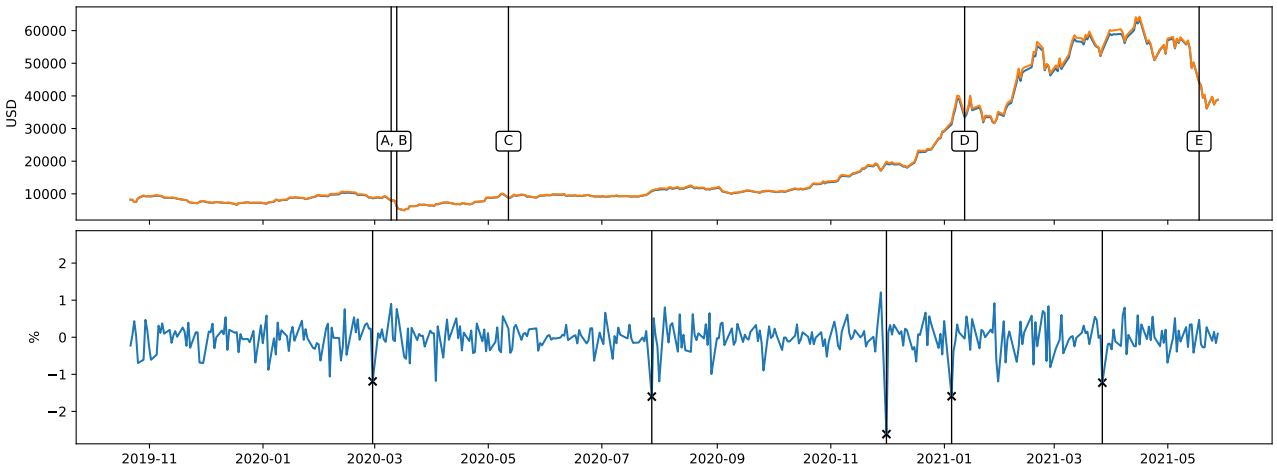

Figure 3: Out-of-sample BTC and BTCF price. The first panel presents the price of BTC in blue line and that of BTCF in orange line. The black vertical lines with capital letter labels indicate the five most negative daily return of BTC in the out-of-sample data. The second panel presents the difference between the % return of BTC and BTCF. The black vertical lines indicate the five most negative returns. The crosses locate the level the returns.

Label	Date	% Drop in Price	Summary
A	2020-03-09	13.83	Coronavirus outbreak that affect the global markets; BTC as potential safe-haven was questioned.[1]
B	2020-03-12	22.89	Continuation of the 2020-03-09 drop.
C	2020-05-11	12.11	Price correction (from \$10,000 to \$8,100) after BTC price surge because of the third supply halving.[2,3]
D	2021-01-11	14.41	Short term correction of BTC hits the \$40,000 mark.[4]
E	2021-05-17	11.86	Tesla stopped taking BTC as payment due to environmental concerns about energy use to process transaction.[5]

Table 1: Summary of events that associated with the five most negative daily price drops in out-of-sample BTC price data. The capital letter labels in the first column are the labels in the first panel of figure 3. [1] is reported by the CNBC news `https://cnb.cx/3HZ2x7K`; [2] is from Forbes `https://bit.ly/3rdJPmP`; [3] is from livemint.com `https://bit.ly/3FRi6Na`; [4] is from CNBC `https://cnb.cx/3nU0ppO`; [5] is from Reuters `https://reut.rs/3leCiAv`.

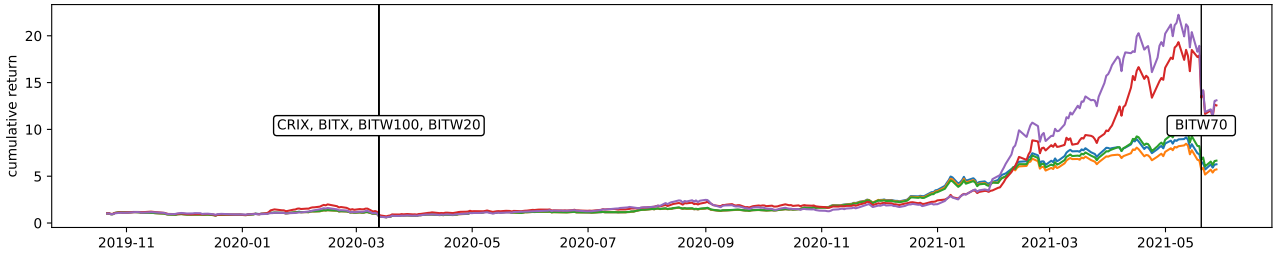

Figure 4: Out-of-sample cumulative return of crypto indices. The black vertical lines indicate largest price drop of indices indicated by the labels. The colouring is as follows: Blue line is CRIX; Orange line is BITX; Green line is BITW100; Red line is BITW20; Purple line is BITW70.

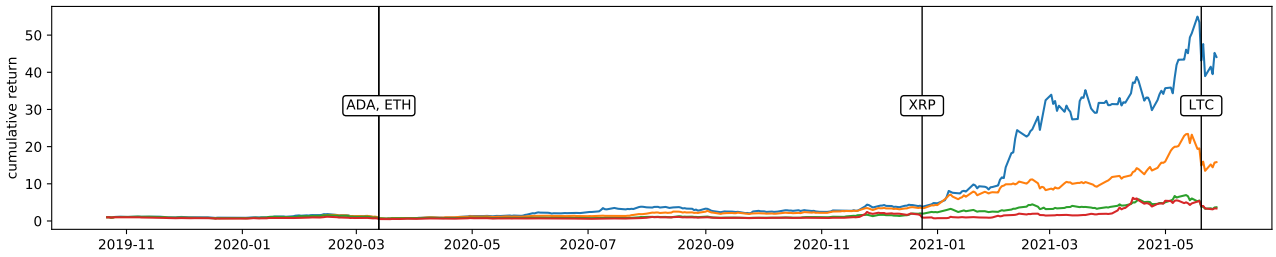

Figure 5: Out-of-sample cumulative return of individual cyptos. The black vertical lines indicate largest price drop of cryptos indicated by the labels. Blue line is ADA; Orange line is ETH; Green line is LTC; Red line is XRP.

Label	Date	% Drop in Price	Summary
CRIX	2020-03-09	23.77	Coronavirus outbreak that affect the global markets including the crpyto market.
BITX		23.68	
BITW100		23.87	
BITW20		26.66	
ADA		23.55	
ETH		27.40	
BITW70	2021-05-19	27.64	The spillover of the BTC shock on 2021-05-17 (label A in figure 3 and table 1)
XRP	2020-12-23	41.00	Top executives were sued by the SEC of misleading investors[1].

Table 2: Summary of events that associated with largest price drops in out-of-sample data. The labels in the first column are the labels in figure 4 and figure 5. CRIX, BITX, BITW100, BITW20, ADA and ETH have the same date the reason of the largest drop. [1] is reported by Bloomberg `https://bloom.bg/3cWdita`.

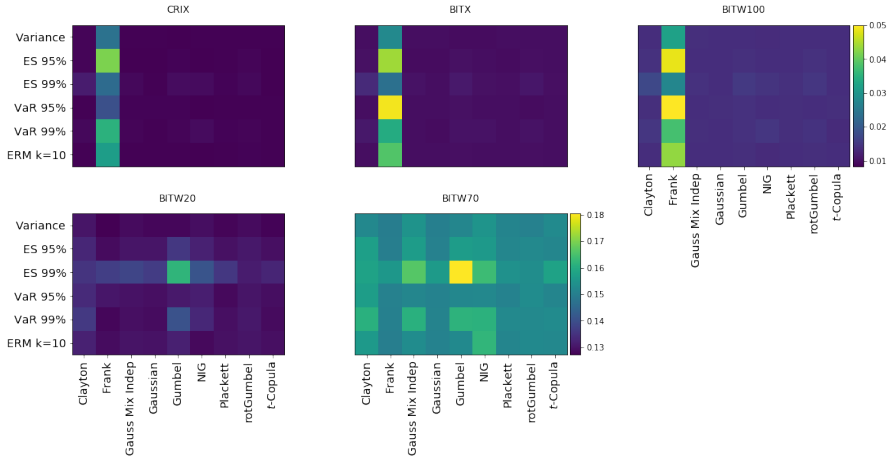

Figure 6: Out-of-sample mean square errors of indices' hedge portfolios. Plots in a row share the same colour scale for comparison.

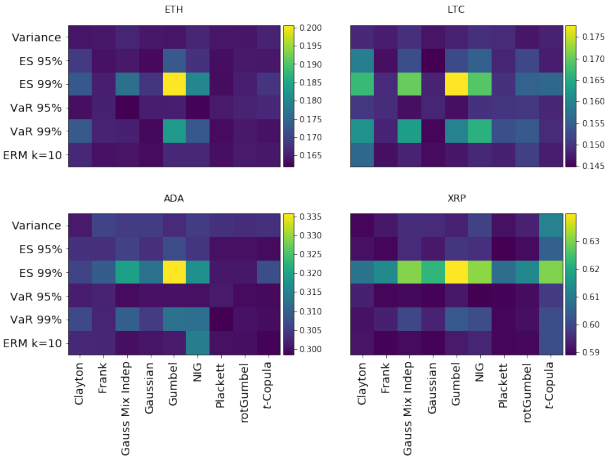

Figure 7: Out-of-sample mean square errors of cryptos' hedge portfolios. Each plot has its own colour scale.

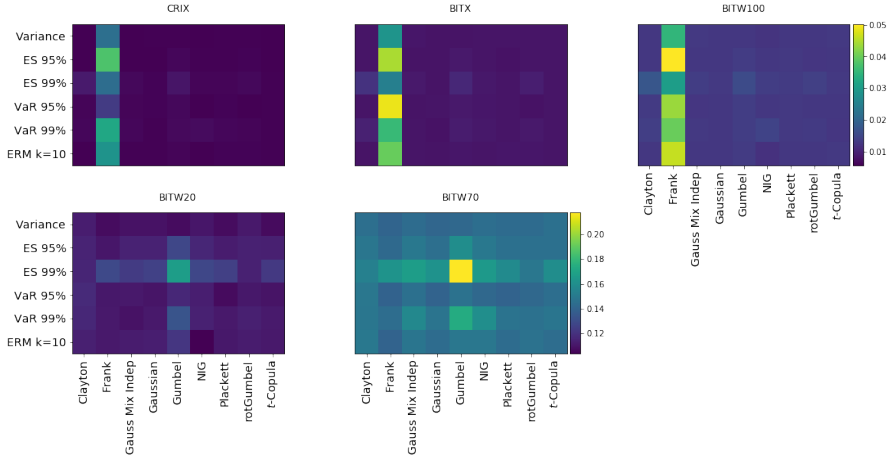

Figure 8: Out-of-sample lower semi variance of indices' hedge portfolios. Plots in a row share the same colour scale for comparison.

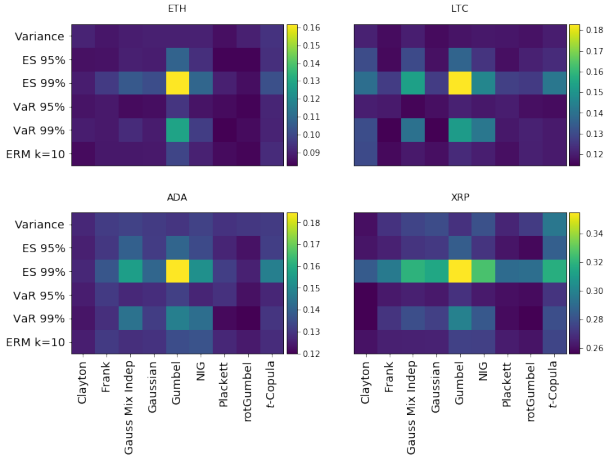

Figure 9: Out-of-sample lower semi variance of cryptos' hedge portfolios. Each plot has its own colour scale.

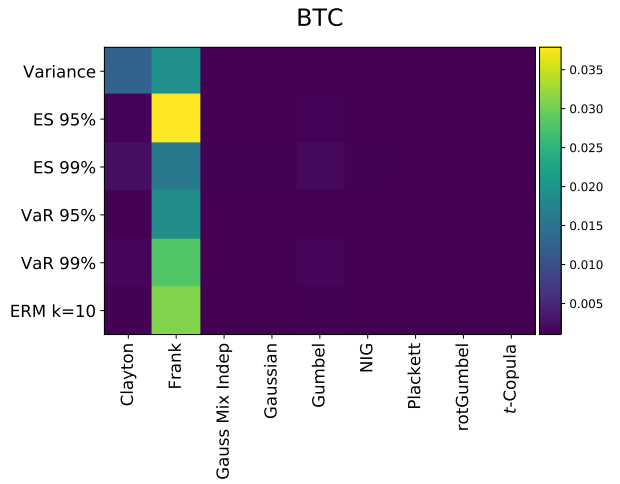

Figure 10: Out-of-sample mean square errors of BTC-BTCF portfolios constructed with different copula and risk minimization objectives. The Frank copula is inferior in the BTC-involved portfolios.

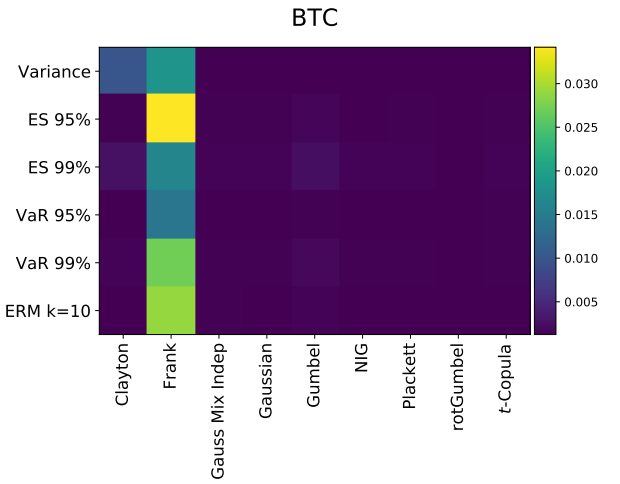

Figure 11: Out-of-sample lower semivariance of BTC-BTCF portfolios constructed with different copula and risk minimization objectives. The Frank copula is obviously inferior.

First, we analyse the results of hedged portfolios without the copula selection step in order to get a better understanding of how a copula affects the hedged portfolio with various risk minimization objectives. To do so, we inspect the hedge performance of copulas by the mean square error and lower semi-variance. The mean square error is the distance between a perfect hedge and the hedged portfolio returns $\text{MSE} = \mathbb{E}(R^2)$. The lower semi-variance is defined as $\text{LSV} = \mathbb{E}\left((R - \mathbb{E}(R))^2 \mathbf{1}_{\{R \leq \mathbb{E}(R)\}}\right)$. All results presentedd here are out-of-sample results obtained without the copula selection step in order to compare the performances across copulae.

Figure 10 and 11 are the mean square error and lower semivariance of BTC-BTCF. We can see that the Frank copula is the worst performing copula: the resulting hedged portfolio returns is far away from a perfect hedge. In Figures 6 and 8, the phenomenom of Frank copula being inferior to its counterparts can be observed from the results of the CRIX, BITX, BITW100, and BITW20-BTCF portfolios. Interestingly, the spot in those portfolios usually have a strong dependence with the BTCF. In contrast, the inferiority of the Frank copula is less prominent in the BITW70, ADA, ETH, LTC and XRP-BTCF portfolios. We suspect that the Frank copula is not a choice to model assets with strong dependence.

We can also observe from Figures 7 and 9 that the Gumbel copula is not performing as well as other copulas in the ETH, LTC, and XRP-BTCF portfolios. The reason is the Gumbel copula has only upper tail dependence, while the ETH, LTC, and XRP exhibit lower tail dependence with BTCF. We will discuss this in the following section.

4.4 Copula Selection Results

Next, we inspect the copula selection result by the AIC procedure described in section 3.2.3. Although the copula selection is only an intermediate step to obtain the OHRs, the result of this step can help us better understand the dependence feature between BTCF and the assets we study in this work. This gives us valuable information to model the assets in the future. Decisions of the AIC procedure are summarised in Table 3.

Overall, the t-copula, rotated Gumbel (rotGumbel), and the NIG factor copula are the most frequently chosen copulae by the AIC procedure.

Spot/ Copula	t	Plackett	GMI	rotGumbel	NIG
Individual Cryptos					
BTC	73	4	2	1	31
ETH	3	6	8	94	1
ADA	0	0	0	0	112
LTC	13	0	3	32	64
XRP	0	31	3	78	0
Crypto Indices with BTC Constituent					
BITX	39	0	14	16	12
CRIX	47	0	11	3	27
BITW100	42	0	8	29	2
Crypto Indices without BTC Constituent					
BITW20	0	0	0	78	3
BITW70	0	0	0	80	1

Table 3: Copula selection results (shortened). The values are the counts of a copula chosen by the AIC procedure during the out-of-sample period. Each count represents five trading days since the each testing data consists of five trading days. The table shows only the frequently chosen copula, i.e. t, Plackett, Gaussian Mix Independent (GMI), rotated Gumbel (rotGumbel), and Normal Inverse Gaussian factor copula (NIG).

The t-copula is frequently chosen to model the dependence between the BTC and BTC-involving-indices, CRIX, BITX, BITW100, and the BTC future. BTC and BTC-involving-indices exhibit strong (upper and lower) tail dependence with BTCF. We interpret tail dependence as a strong tendency for one asset to be extreme when another is extreme and vice versa (McNeil et al., 2015). In fact, the t copula has been recommended in various empirical studies to model financial data, such as Zeevi and Mashal (2002) and Breymann et al. (2003). Those studies suggest that the t-copula is a better model compared to the Gaussian copula as financial data typically exhibit heavy tails and tail dependence.

On the other hand, the radial symmetry of the t-copula appears to be a poor choice to model the remaining hedging pairs. Demarta and McNeil (2005) describe the radial symmetry feature of the t-copula "strong" as it is a radially symmetric distribution. To be specific, if $(U_1, ..., U_d)$ is a vector distributed in t-copula, then $(U_1, ..., U_d) \stackrel{\mathcal{L}}{=} (1 - U_1, ..., 1 - U_d)$. This symmetry can be justified in the dependence structure between a futures and its underlying by the theory of futures pricing, which suggests the price of a futures is a function of the underlying price (Hull, 2003). However, there is no such relationship between a futures and an asset which is not the underlying. Besides, asset prices tend to crash simultaneously whereas positive development tends to be idiosyncratic.

Among the three popular copulae, rotGumbel copula shows its ability to model the dependence between ETH and BTCF. rotGumbel also performs well when modelling dependence between XRP, BITW20, BITW70, and the BTCF. In particular, the whole time series of the two indices, BITW20 and BITW70, are best fitted solely with the rotated Gumbel copula.

In fact, Clayton's AIC in many of the training sets is the second lowest, just higher than that of rotated Gumbel. This is because the Clayton copula has the same ability to model the lower quantile dependence. However, Clayton's radial like feature does not match the behaviour of the financial data.

It is worth to mention that although the NIG factor copula is penalised heavily due to its three parameters setup, it is frequently chosen to be the best copula to model the dependence between

individual cryptos and the BTC future. An extreme case would be ADA, where only NIG factor is chosen in our dataset. Another dependence structure being best described by the NIG factor copula is the pair of LTC-BTCF, with 64 out of 112 training sets best fitted by the NIG factor copula. Indices like BITX and CRIX are sometimes best fitted with the NIG factor copula as well, accounting for modelling 12 and 27 training sets respectively. The popularity of the NIG factor copula reflects the ability of the copula to model very complex dependence structure: the NIG factor copula is able to model the tail, radial asymmetry.

The Frank copula is generally not a good choice to model financial data (as also reported by Barbi and Romagnoli (2014)). Plackett is characterised by its dependence parameter being equal to the cross-product ratio, see eq. 9. However, apparently, this property does not capture the dependence structure of cryptos and BTCF.

4.5 Hedged portfolios with the copula selection step

Table 4 presents the first two moments, maximum drawdown (MD) and the date of MD of the hedge portfolios. We observe that the statistics of the portfolios with different objectives are similar to each other. We provide the detail in Tables 6 to 11 in the appendix.

Unsurprisingly, the BTC-involved spots, i.e. BTC, CRIX, BITX, and BITW100, are well hedged by the BTCF regardless of risk minimization objective. Contrarily, BTC-not-involved spots' portfolios are less promising. Those hedge portfolios' returns are as volatile as the assets, see for example ADA and XRP. We will further discuss the effectiveness of hedge in the next section.

4.6 Hedging Effectiveness Results

In this section, we analyse the out-of-sample hedging effectiveness (HE) of BTCF as hedging. HE is defined as

$$\text{HE} = 1 - \frac{\rho_h}{\rho_s},$$

a measure of the percentage reduction of portfolio risk attribute, in our case the spot ρ_s, to hedged portfolio risk attribute ρ_h. A higher HE indicates a greater risk reduction and thus the hedge is more effective.

The HE above is a generalisation of how Ederington (1979) evaluate hedging performance. In addition to variance, we include the risk measures which act as loss function while searching for OHR: ES 95% and 99%, VaR 95% and 99% and ERM.

The formulation above gives a point estimate per testing data. However, each of our test data contain only 5 data points, the length is not sufficient to draw meaningful risk measure results. To address this issue, we apply bootstrapping method on the concatenated test data time series as described in the beginning of the result section.

The bootstrapping method is known to be a powerful nonparametric tool for approximating complicated statistics (Efron and Tibshirani, 1994; Davison and Hinkley, 1997). We apply stationary block bootstrapping to the time series introduced by Politis and Romano (1994) in our analysis in order to preserve the temporal structure of the data while sampling. The configuration of stationary bootstrapping procedure in this work is as follows. Assume a time series with N observations $\{X_t\}_{t\in[1,N]}$ is a strong stationary, weakly dependence time series of interest, we form blocks of samples $B = \{X_i, ..., X_{i+j-1}\}$. Index i is a random variable uniformly distributed over $[1, 2, ..., N]$ and j is geometric distributed random variable with parameter p. The block index i and block length j are

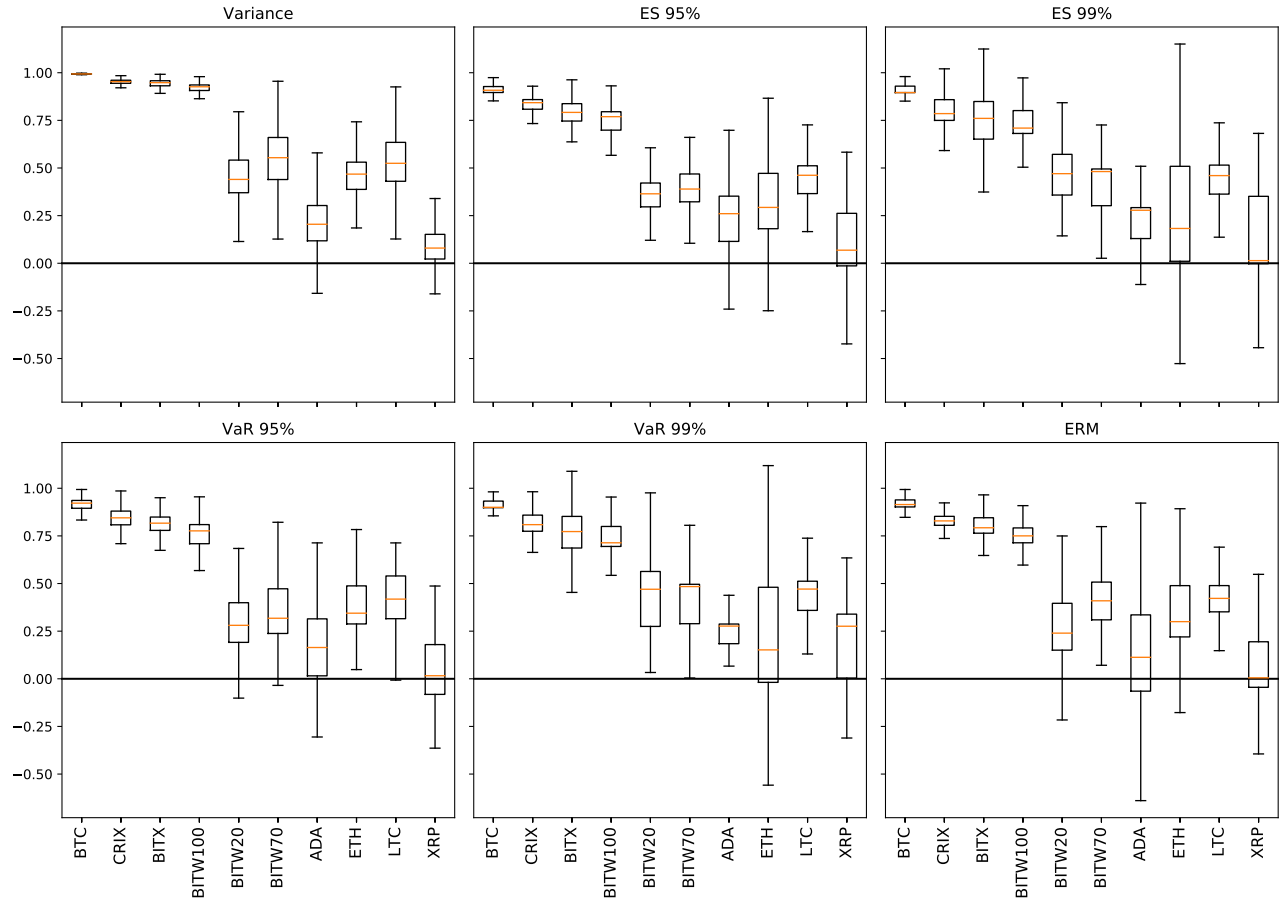

Figure 12: Hedging effectiveness (HE) of portfolios with different risk minimization objectives evaluated by the corresponding risk minimization objectives. The boxplots indicate the the median, upper quartile, lower quartile, minimium and maximum of the bootstrapped HE. The HE of BTC-involved spots are significantly higher than that of BTC-not-involved spots.

independent. For any index k which is greater than N, the sample X_k is defined to be $X_{k(\mod N)}$. For each block, we calculate the hedging effectiveness with different risk measures mentioned above. We choose $p = 1/250$, implying the average block length is 250. This average block length is chosen to reasonably calculate ES and VaR. 100 blocks are drawn for each risk minimising objective and spot.

Figure 12 report the bootstrapped HE samples from the concatenated out-of-sample hedge portfolio return. As expected, the BTC involving spots, the BTC, CRIX, BITX and BITW100, are well hedged by the BTCF. The HEs of BTCF to other cryptos and indices are substantially lower than to the BTC involving spots, but the consistency the performances across different risk reduction objectives and HE evaluation remains.

Some HE bootstrapping samples are negative, it means that it is possible that introducing the BTC futures increases risk of the portfolios. This is an unfavorable situation for investors if they want to hedge cryptos with BTC futures. We do not recommend BTC futures being used to cross hedge cryptos.

	BTC	ETH	ADA	LTC	XRP	BITX	CRIX	BITW100	BITW20	BITW70
Assets										
Mean %	0.3915	0.6819	0.9467	0.3227	0.2987	0.4308	0.4602	0.4683	0.6249	0.6353
Std %	4.4023	6.0103	6.699	6.4781	7.9843	4.5676	4.542	4.6174	5.5021	5.8155
MD %	-25.9965	-32.0144	-26.8528	-37.5913	-52.7652	-27.022	-27.1385	-27.2694	-31.0092	-32.3453
MD date	2020-03-12	2020-03-12	2020-03-12	2021-05-19	2020-12-23	2020-03-12	2020-03-12	2020-03-12	2020-03-12	2021-05-19
Variance minimizing portfolios										
Mean %	0.0215	0.2823	0.5617	-0.0871	-0.0123	0.0561	0.0812	0.0855	0.2429	0.2706
Std %	0.3221	3.8741	5.2722	3.9052	7.1537	0.9954	0.9183	1.1986	3.5846	3.8838
MD %	-1.4393	-17.7421	-13.8687	-28.3029	-52.5236	-7.7567	-7.1025	-11.3866	-21.468	-23.9984
MD date	2020-11-30	2021-05-19	2021-01-08	2021-05-19	2020-12-23	2021-05-19	2021-05-19	2021-05-19	2021-05-19	2021-05-19
VaR 95% minimizing portfolios										
Mean %	0.0253	0.3084	0.5726	-0.0742	0.0208	0.0562	0.0863	0.0846	0.2728	0.2847
Std %	0.3294	3.8944	5.2204	3.9145	7.152	0.993	0.9151	1.198	3.594	3.9133
MD %	-1.5347	-19.175	-14.6974	-28.3672	-52.5667	-7.5639	-6.9744	-11.2582	-22.0733	-24.6513
MD date	2020-11-30	2021-05-19	2021-05-19	2021-05-19	2020-12-23	2021-05-19	2021-05-19	2021-05-19	2021-05-19	2021-05-19
VaR 99% minimizing portfolios										
Mean %	0.0176	0.2977	0.5562	-0.0852	0.0352	0.0593	0.0738	0.0823	0.2499	0.2788
Std %	0.3270	3.9132	5.3466	4.1503	7.1658	1.0178	0.9695	1.2338	3.621	3.9257
MD %	-1.5689	-18.6061	-15.4795	-29.0915	-52.5727	-8.0299	-7.0185	-11.8752	-21.6634	-24.5294
MD date	2020-11-30	2021-05-19	2021-05-19	2021-05-19	2020-12-23	2021-05-19	2021-05-19	2021-05-19	2021-05-19	2021-05-19
ES 95% minimizing portfolios										
Mean %	0.0204	0.3082	0.5525	-0.0808	0.0176	0.0591	0.0777	0.0848	0.2608	0.2785
Std %	0.3234	3.889	5.2673	3.9829	7.1533	1.0065	0.9207	1.2125	3.6115	3.9157
MD %	-1.5629	-18.7819	-14.9647	-28.4608	-52.5698	-7.6211	-6.9894	-11.1357	-21.543	-24.3474
MD date	2020-11-30	2021-05-19	2021-05-19	2021-05-19	2020-12-23	2021-05-19	2021-05-19	2021-05-19	2021-05-19	2021-05-19
ES 99% minimizing portfolios										
Mean %	0.0148	0.308	0.5016	-0.1029	-0.02	0.0598	0.0835	0.0781	0.2538	0.266
Std %	0.3476	3.8954	5.404	4.1581	7.2887	1.0312	0.9461	1.264	3.6323	3.932
MD %	-1.6225	-18.7625	-15.4481	-29.1727	-52.57	-7.7424	-7.0203	-11.9263	-21.9866	-24.4764
MD date	2020-11-30	2021-05-19	2021-05-19	2021-05-19	2020-12-23	2021-05-19	2021-05-19	2021-05-19	2021-05-19	2021-05-19
ERM $k = 10$ minimizing portfolios										
Mean %	0.0223	0.3117	0.5722	-0.0512	0.0155	0.059	0.084	0.0853	0.2564	0.2818
Std %	0.3221	3.8679	5.359	3.8812	7.1579	1.0078	0.9087	1.2032	3.6009	3.9074
MD %	-1.5242	-18.8729	-14.3885	-28.0879	-52.5689	-7.8581	-7.053	-11.1846	-21.592	-24.525
MD date	2020-11-30	2021-05-19	2021-01-08	2021-05-19	2020-12-23	2021-05-19	2021-05-19	2021-05-19	2021-05-19	2021-05-19

Table 4: First two moments, maximum downdown (MD) and date fo MD of assets and hedge portfolios out-of-sample return.

5 Data Availability Statement

The data and codes that support the findings of this study are available in a github repository https://bit.ly/3IVsMMK.

6 Conclusion and Outlook

We study the effectiveness of hedging cryptos and crypto indices with Bitcoin futures. To accomodate different risk appetites and scenarios, a variety of commonly used risk measures are considered to determine the optimal hedge ratio. The risk measures comprise variance, value-at-risk at the confidence levels 95% and 99%, expected shortfall 95% and 99%, and the exponential risk measure with parameter $k = 10$.

At the time of writing, the crypto market is a vibrant and fast-developing market, causing cryptos to have complex and time-changing dependence structures with the Bitcoin futures. As a consequence, the dependence between the cryptos and the futures contract plays an important role in hedging as it determines the distribution of the portfolio returns. We therefore consider various copulae, a flexible statistical tool that separates modelling of the marginals and the dependence structure of multivariate random vectors. To address the potential time-changing dependence, we periodically re-calibrate the copula models and determine the best-fitting copula via AIC.

An extensive out-of-sample backtest suggests that the Bitcoin futures are consistently capable of hedging BTC and BTC-involved indices, i.e., BITX, CRIX, and BITW100, under different risk minimisation objectives and copula models. The mean-square errors (MSEs) and lower semi-variances (LSVs) of the resulting portfolios are indistinguishably at a low level except for the Frank copula. On the other hand, the AIC procedure favours the t-copula because it captures the tail dependence feature of the data. Compared to the unhedged cases, the portfolios' out-of-sample maximum drawdowns are significantly reduced.

Contrarily, we observe diverse results of the capability of BTC futures to hedge other cryptos and crypto indices that exclude Bitcoin. In general, ES 95% and VaR 95% perform better than their 99% counterparts. In particular, minimising ES 99% leads to relatively high MSEs and LSVs regardless of the copula in use. The ES 99% and VaR 99% even result in out-of-sample maximum drawdowns that are higher than that of the 95% counterparts in some portfolios, for example in the ETH- and LTC-BTCF portfolio. Therefore, we conclude that overly emphasising tail risks by choosing extreme tail risk measures does not lead to a promising hedge in a cross-hedging setting.

The AIC procedure mainly favours the rotated Gumbel and the NIG factor copula in modelling non-BTC relate cryptos and indices. This reflects the idiosyncratic nature of downward movements in the crypto market. Interestingly, the best-fitting copula does not necessary lead to the best performing portfolio in terms of MSE or LSV. For example, this is the case for ADA. We suspect this discrepancy between the optimal copula selection and MSE-LSV results can be attributed to the static linear nature of the hedge, as the sole hedge instrument is a futures contract.

Although copulae are flexible to model complex dependence structures by emphasising a number of important features such as lower tail dependence and radial symmetry, the simple linear hedge is very limited in its flexibility to address this complex dependence. Including liquidly traded derivatives with non-linear payoffs, such as options, might be a possibility to improve the hedge quality for these cryptos and portfolios.

References

Acerbi, C. (2002): "Spectral measures of risk: A coherent representation of subjective risk aversion," *Journal of Banking & Finance*, 26, 1505–1518.

Akaike, H. (1973): "Information theory and an extension of the maximum likelihood principle," in *Second International Symposium on Information Theory*, ed. by B. N. Petrov and F. Csaki, Budapest: Akadémiai Kiado, 267–281.

Anderson, D., K. Burnham, and G. White (1998): "Comparison of Akaike information criterion and consistent Akaike information criterion for model selection and statistical inference from capture-recapture studies," *Journal of Applied Statistics*, 25, 263–282.

Artzner, P., F. Delbaen, J.-M. Eber, and D. Heath (1999): "Coherent measures of risk," *Mathematical Finance*, 9, 203–228.

Barbi, M. and S. Romagnoli (2014): "A Copula-Based Quantile Risk Measure Approach to Estimate the Optimal Hedge Ratio," *Journal of Futures Markets*, 34, 658–675.

Barndorff-Nielsen, O. E. (1997): "Normal inverse Gaussian distributions and stochastic volatility modelling," *Scandinavian Journal of statistics*, 24, 1–13.

Breymann, W., A. Dias, and P. Embrechts (2003): "Dependence structures for multivariate high-frequency data in finance," .

Cherubini, U., S. Mulinacci, and S. Romagnoli (2011): "A copula-based model of speculative price dynamics in discrete time," *Journal of Multivariate Analysis*, 102, 1047–1063.

Cont, R. (2001): "Empirical properties of asset returns: stylized facts and statistical issues," *Quantitative Finance*, 1, 223–236.

Davison, A. C. and D. V. Hinkley (1997): *Bootstrap methods and their application*, 1, Cambridge university press.

Demarta, S. and A. J. McNeil (2005): "The t copula and related copulas," *International statistical review*, 73, 111–129.

Dowd, K., J. Cotter, and G. Sorwar (2008): "Spectral risk measures: properties and limitations," *Journal of Financial Services Research*, 34, 61–75.

Ederington, L. H. (1979): "The hedging performance of the new futures markets," *The journal of finance*, 34, 157–170.

Efron, B. and R. J. Tibshirani (1994): *An introduction to the bootstrap*, CRC press.

Embrechts, P., A. McNeil, and D. Straumann (2002): "Correlation and dependence in risk management: properties and pitfalls," *Risk management: value at risk and beyond*, 1, 176–223.

Fama, E. F. (1963): "Mandelbrot and the stable Paretian hypothesis," *The Journal of Business*, 36, 420–429.

Fisher, N. I. and P. K. Sen (2012): *The collected works of Wassily Hoeffding*, Springer Science & Business Media.

Föllmer, H. and A. Schied (2002): *Stochastic Finance. An Introduction in Discrete Time*, de Gruyter.

Genest, C. (1987): "Frank's family of bivariate distributions," *Biometrika*, 74, 549–555.

Genest, C., K. Ghoudi, and L.-P. Rivest (1995): "A semiparametric estimation procedure of dependence parameters in multivariate families of distributions," *Biometrika*, 82, 543–552.

Genest, C. and L.-P. Rivest (1993): "Statistical inference procedures for bivariate Archimedean copulas," *Journal of the American statistical Association*, 88, 1034–1043.

Härdle, W. K., N. Hautsch, and L. Overbeck (2008): *Applied Quantitative Finance*, Springer Science & Business Media.

Härdle, W. K., M. Müller, S. Sperlich, and A. Werwatz (2004): *Nonparametric and Semiparametric Models*, Springer Science & Business Media.

Härdle, W. K. and O. Okhrin (2010): "De copulis non est disputandum," *AStA Advances in Statistical Analysis*, 94, 1–31.

Härdle, W. K. and L. Simar (2019): *Applied multivariate statistical analysis Fifth Edition*, Springer.

Hoeffding, W. (1940a): "Masstabinvariante Korrelationstheorie," *Schriften des Mathematischen Instituts und Instituts fur Angewandte Mathematik der Universitat Berlin*, 5, 181–233.

——— (1940b): "Scale-invariant correlation theory (English translation)," 5, 181–233.

——— (1941): "Scale-invariant correlations for discontinuous distributions (English translation)," 7, 49–70.

Hull, J. C. (2003): *Options futures and other derivatives*, Pearson Education India.

Joe, H. (1997): *Multivariate models and multivariate dependence concepts*, CRC Press.

Kalemanova, A., B. Schmid, and R. Werner (2007): "The normal inverse Gaussian distribution for synthetic CDO pricing," *The Journal of Derivatives*, 14, 80–94.

Krupskii, P. and H. Joe (2013): "Factor copula models for multivariate data," *Journal of Multivariate Analysis*, 120, 85–101.

Kruskal, W. H. (1958): "Ordinal measures of association," *Journal of the American Statistical Association*, 53, 814–861.

McNeil, A., R. Frey, and P. Embrechts (2005): *Quantitative Risk Management*, Princeton, NJ: Princeton University Press.

——— (2015): *Quantitative Risk Management*, Princeton, NJ: Princeton University Press, 2nd ed.

Menezes, C., C. Geiss, and J. Tressler (1980): "Increasing downside risk," *The American Economic Review*, 70, 921–932.

Nakamoto, S. (2009): "Bitcoin: A Peer-to-Peer Electronic Cash System," .

Nelsen, R. (2002): "Concordance and copulas: A survey," in *Distributions with Given Marginals and Statistical Modelling*, Kluwer Academic Publishers, 169–178.

Nelsen, R. B. (1999): *An Introduction to Copulas*, Springer.

Politis, D. N. and J. P. Romano (1994): "The Stationary Bootstrap," *Journal of the American Statistical Association*, 1303–1313.

Schweizer, B., E. F. Wolff, et al. (1981): "On nonparametric measures of dependence for random variables," *Annals of Statistics*, 9, 879–885.

Sklar, A. (1959): "Fonctions de répartition a n dimensions et leurs marges," *Publications de l'Institut de Statistique de l'Universite de Paris*, 8, 229–231.

Takeuchi, K. (1976): "Distribution of informational statistics and a criterion of model fitting. Suri-Kagaku (Mathematical Sciences) 153 12-18," .

Zeevi, A. and R. Mashal (2002): "Beyond correlation: Extreme co-movements between financial assets," *Available at SSRN 317122*.

A Density of linear combination of random variables

Proposition 6 *Let $\boldsymbol{X} = (X_1, ..., X_d)^\top$ be real-valued random variables with corresponding copula density $\boldsymbol{c}_{X_1,...,X_d}$, and continuous marginals $F_{X_1}, ..., F_{X_d}$. Then, the pdf of the linear combination of marginals $Z = n_1 \cdot X_1 + ... + n_d \cdot X_d$ is*

$$f_Z(z) = \left|n_1^{-1}\right| \int_{[0,1]^{d-1}} \boldsymbol{c}_{X_1,...,X_d}\left(F_{X_1}(S(z)), u_2, ..., u_d\right) \cdot f_{X_1}(S(z)) \mathrm{d}u_2 ... \mathrm{d}u_d \tag{10}$$

$$S(z) = \frac{1}{n_1} \cdot z - \frac{n_2}{n_1} \cdot F_{X_2}^{(-1)}(u_2) - ... - \frac{n_d}{n_1} \cdot F_{X_d}^{(-1)}(u_d).$$

Proof. Let $Z = n_1 \cdot X_1 + ... + n_d \cdot X_d$ and let $\mathbf{A} = \begin{bmatrix} n_1 & n_2 & \cdots & n_d \\ 0 & 1 & \cdots & 0 \\ \vdots & & \ddots & \vdots \\ 0 & \cdots & & 1 \end{bmatrix}$. Then,

$$\begin{bmatrix} Z \\ X_2 \\ \vdots \\ X_d \end{bmatrix} = \boldsymbol{A} \begin{bmatrix} X_1 \\ X_2 \\ \vdots \\ X_d \end{bmatrix}.$$

By transformation of the variables (Härdle and Simar, 2019)

$$\begin{aligned} \boldsymbol{f}_{Z,X_2,...,X_d}(z, x_2, ..., x_d) &= \boldsymbol{f}_{X_1,...,X_d}\left(\boldsymbol{A}^{-1} \begin{bmatrix} z \\ x_2 \\ \vdots \\ x_d \end{bmatrix}\right) \cdot \left|\det \boldsymbol{A}^{-1}\right| \\ &= \left|n_1^{-1}\right| \boldsymbol{f}_{X_1,...,X_d}\left(S(z), x_2, ..., x_d\right). \end{aligned}$$

Let $u_i = F_{X_i}(x_i)$ and by chain rule we have

$$\begin{aligned} \boldsymbol{f}_{X_1,...,X_d}(x_1, ..., x_d) &= \frac{\partial^d F_{X_1,...,X_d}(x_1, ..., x_d)}{\partial x_1 ... \partial x_d} \\ &= \boldsymbol{c}_{X_1,...,X_d}(u_1, ..., u_d) \cdot \prod_{i=1}^{d} f_{X_i}(x_i). \end{aligned}$$

Therefore,

$$\begin{aligned} &\boldsymbol{f}_{Z,X_2,...,X_d}(z, x_2, ..., x_d) = \\ &\quad \left|n_1^{-1}\right| \cdot \boldsymbol{c}_{X_1,...,X_d}\left(F_{X_1}(S(z)), u_2, ..., u_d\right) \cdot f_{X_1}\{S(z)\} \cdot \prod_{i=2}^{d} f_{X_i}(x_i). \end{aligned}$$

The claim (10) is obtained by integrating out $x_2, ...x_d$ by substituting $\mathrm{d}x_i = \frac{1}{f_{X_i}(x_i)} \mathrm{d}u_i$. ■

B Summary Statistics of Assets

	Mean %	Std %	Skew	Kurt	MD %	MD date	ρ	τ
Hedging Instrument								
BTCF	0.3906	4.6312	-0.5060	4.4204	-26.9920	2020-03-12	1.0000	1.0000
Individual Cryptos								
BTC	0.3915	4.4023	-0.5857	4.6565	-25.9965	2020-03-12	0.9975	0.9507
ETH	0.6819	6.0103	-0.2557	5.2646	-32.0144	2020-03-12	0.7712	0.5988
ADA	0.9467	6.6990	0.1661	2.3086	-26.8528	2020-03-12	0.6296	0.4825
LTC	0.3227	6.4781	-0.9935	5.3011	-37.5913	2021-05-19	0.8080	0.6113
XRP	0.2987	7.9843	0.5542	12.4882	-52.7652	2020-12-23	0.4510	0.4939
Crypto Indices with BTC Constituent								
BITX	0.4308	4.5676	-0.8842	4.7222	-27.0220	2020-03-12	0.9769	0.8738
CRIX	0.4602	4.5420	-0.7952	4.7549	-27.1385	2020-03-12	0.9799	0.8769
BITW100	0.4683	4.6174	-0.9864	4.9381	-27.2694	2020-03-12	0.9674	0.8537
Crypto Indices without BTC Constituent								
BITW20	0.6249	5.5021	-1.1518	5.2203	-31.0092	2020-03-12	0.7674	0.5883
BITW70	0.6353	5.8155	-1.1171	5.1926	-32.3453	2021-05-19	0.7525	0.5459

Table 5: Summary statistics of assets' daily returns during the out-of-sample period, from 2019-10-21 to 2021-05-27. The first four columns are the first four moments of assets' daily returns. The fifth and sixth columns are the maximum drawdown (MD) and the date of the MD. The last two columns are Pearson's ρs and Kendall's τs between the assets and BTCF.

C Summary Statistics of Hedged Portfolios

	Mean %	Std %	Skew	Kurt	MD %	MD date	Variance
Individual Cryptos							
BTC	0.0215	0.3221	-1.0119	3.1929	-1.4393	2020-11-30	0.0000
ETH	0.2823	3.8741	0.9469	7.1064	-17.7421	2021-05-19	0.0015
ADA	0.5617	5.2722	1.3634	4.4818	-13.8687	2021-01-08	0.0028
LTC	-0.0871	3.9052	-0.3617	7.6239	-28.3029	2021-05-19	0.0018
XRP	-0.0123	7.1537	1.1451	20.0236	-52.5236	2020-12-23	0.0043
Crypto Indices with BTC Constituent							
BITX	0.0561	0.9954	-0.4204	13.2487	-7.7567	2021-05-19	0.0001
CRIX	0.0812	0.9183	-0.0027	14.3136	-7.1025	2021-05-19	0.0001
BITW100	0.0855	1.1986	-1.7440	22.2644	-11.3866	2021-05-19	0.0001
Crypto Indices without BTC Constituent							
BITW20	0.2429	3.5846	-0.3063	4.1622	-21.4680	2021-05-19	0.0013
BITW70	0.2706	3.8838	-0.6490	4.6312	-23.9984	2021-05-19	0.0015

Table 6: Summary statistics of out-of-sample daily returns of hedged portfolios that minimize variance.

	Mean %	Std %	Skew	Kurt	MD %	MD date	VaR 5%
Individual Cryptos							
BTC	0.0253	0.3294	-0.9725	3.4373	-1.5347	2020-11-30	0.0063
ETH	0.3084	3.8944	1.0243	7.4297	-19.1750	2021-05-19	0.0514
ADA	0.5726	5.2204	1.2981	4.2544	-14.6974	2021-05-19	0.0769
LTC	-0.0742	3.9145	-0.3836	7.5384	-28.3672	2021-05-19	0.0622
XRP	0.0208	7.1520	1.1269	19.8930	-52.5667	2020-12-23	0.0683
Crypto Indices with BTC Constituent							
BITX	0.0562	0.9930	-0.3117	12.4780	-7.5639	2021-05-19	0.0128
CRIX	0.0863	0.9151	0.0718	13.7915	-6.9744	2021-05-19	0.0092
BITW100	0.0846	1.1980	-1.6592	21.3725	-11.2582	2021-05-19	0.0164
Crypto Indices without BTC Constituent							
BITW20	0.2728	3.5940	-0.3721	4.4896	-22.0733	2021-05-19	0.0546
BITW70	0.2847	3.9133	-0.6580	4.7874	-24.6513	2021-05-19	0.0626

Table 7: Summary statistics of out-of-sample daily returns of hedged portfolios that minimize VaR 5%.

	Mean %	Std %	Skew	Kurt	MD %	MD date	VaR 1%
Individual Cryptos							
BTC	0.0176	0.3270	-1.0405	3.3742	-1.5689	2020-11-30	0.0134
ETH	0.2977	3.9132	0.9547	7.2414	-18.6061	2021-05-19	0.1026
ADA	0.5562	5.3466	1.1362	3.9334	-15.4795	2021-05-19	0.1106
LTC	-0.0852	4.1503	-0.7234	7.3208	-29.0915	2021-05-19	0.1030
XRP	0.0352	7.1658	1.1582	19.8506	-52.5727	2020-12-23	0.1387
Crypto Indices with BTC Constituent							
BITX	0.0593	1.0178	-0.5331	13.3100	-8.0299	2021-05-19	0.0247
CRIX	0.0738	0.9695	-0.4729	13.6500	-7.0185	2021-05-19	0.0245
BITW100	0.0823	1.2338	-1.9365	23.1938	-11.8752	2021-05-19	0.0347
Crypto Indices without BTC Constituent							
BITW20	0.2499	3.6210	-0.3866	4.3396	-21.6634	2021-05-19	0.0988
BITW70	0.2788	3.9257	-0.7635	5.1288	-24.5294	2021-05-19	0.1147

Table 8: Summary statistics of out-of-sample daily returns of hedged portfolios that minimize VaR 1%.

	Mean %	Std %	Skew	Kurt	MD %	MD date	ES 5%
Individual Cryptos							
BTC	0.0204	0.3234	-1.0150	3.4423	-1.5629	2020-11-30	0.0101
ETH	0.3082	3.8890	1.0119	7.4077	-18.7819	2021-05-19	0.0782
ADA	0.5525	5.2673	1.2557	4.2423	-14.9647	2021-05-19	0.0984
LTC	-0.0808	3.9829	-0.4957	7.2302	-28.4608	2021-05-19	0.0962
XRP	0.0176	7.1533	1.1411	19.9176	-52.5698	2020-12-23	0.1354
Crypto Indices with BTC Constituent							
BITX	0.0591	1.0065	-0.3453	12.1335	-7.6211	2021-05-19	0.0215
CRIX	0.0777	0.9207	0.0164	13.5608	-6.9894	2021-05-19	0.0173
BITW100	0.0848	1.2125	-1.6397	19.7472	-11.1357	2021-05-19	0.0274
Crypto Indices without BTC Constituent							
BITW20	0.2608	3.6115	-0.3555	4.2016	-21.5430	2021-05-19	0.0804
BITW70	0.2785	3.9157	-0.6949	4.8047	-24.3474	2021-05-19	0.0908

Table 9: Summary statistics of out-of-sample daily returns of hedged portfolios that minimize ES 5%.

	Mean %	Std %	Skew	Kurt	MD %	MD date	ES 1%
Individual Cryptos							
BTC	0.0148	0.3476	-0.8354	3.3054	-1.6225	2020-11-30	0.0234
ETH	0.3080	3.8954	0.9840	7.4947	-18.7625	2021-05-19	0.1299
ADA	0.5016	5.4040	1.1008	3.9607	-15.4481	2021-05-19	0.1463
LTC	-0.1029	4.1581	-0.7757	7.4375	-29.1727	2021-05-19	0.1647
XRP	-0.0200	7.2887	1.1121	18.8732	-52.5700	2020-12-23	0.2516
Crypto Indices with BTC Constituent							
BITX	0.0598	1.0312	-0.4410	11.5863	-7.7424	2021-05-19	0.0411
CRIX	0.0835	0.9461	-0.0361	12.4047	-7.0203	2021-05-19	0.0350
BITW100	0.0781	1.2640	-1.9645	21.8836	-11.9263	2021-05-19	0.0593
Crypto Indices without BTC Constituent							
BITW20	0.2538	3.6323	-0.4086	4.4462	-21.9866	2021-05-19	0.1282
BITW70	0.2660	3.9320	-0.7598	5.0050	-24.4764	2021-05-19	0.1535

Table 10: Summary statistics of out-of-sample daily returns of hedged portfolios that minimize ES 1%.

	Mean %	Std %	Skew	Kurt	MD %	MD date	ERM k=10
Individual Cryptos							
BTC	0.0223	0.3221	-1.0008	3.4153	-1.5242	2020-11-30	0.0057
ETH	0.3117	3.8679	1.0345	7.5751	-18.8729	2021-05-19	0.0491
ADA	0.5722	5.3590	1.4203	4.6970	-14.3885	2021-01-08	0.0700
LTC	-0.0512	3.8812	-0.2929	7.7022	-28.0879	2021-05-19	0.0616
XRP	0.0155	7.1579	1.1244	19.8583	-52.5689	2020-12-23	0.0787
Crypto Indices with BTC Constituent							
BITX	0.0590	1.0078	-0.4427	13.0839	-7.8581	2021-05-19	0.0127
CRIX	0.0840	0.9087	0.0488	14.5501	-7.0530	2021-05-19	0.0100
BITW100	0.0853	1.2032	-1.6522	20.5562	-11.1846	2021-05-19	0.0153
Crypto Indices without BTC Constituent							
BITW20	0.2564	3.6009	-0.3446	4.2152	-21.5920	2021-05-19	0.0503
BITW70	0.2818	3.9074	-0.6952	4.8745	-24.5250	2021-05-19	0.0557

Table 11: Summary statistics of out-of-sample daily returns of hedged portfolios that minimize ERM $k = 10$.

IRTG 1792 Discussion Paper Series 2022

For a complete list of Discussion Papers published, please visit http://irtg1792.hu-berlin.de.

001 "Hedging Cryptos with Bitcoin Futures" by Francis Liu, Natalie Packham, Meng-Jou Lu, Wolfgang Karl Härdle, January 2022.

IRTG 1792, Spandauer Strasse 1, D-10178 Berlin
http://irtg1792.hu-berlin.de

This research was supported by the Deutsche Forschungsgemeinschaft through the IRTG 1792.